ISSN 2745-3502
Volume 4 No. 1 – Agustus 2023 *Indonesian Applied Physics Letters*

IMPLEMENTATION OF FAST FOURIER TRANSFORM(FFT) FOR INFANT CRYING DETECTION

Latifah Listyalina [1, a)] Evrita Lusiana Utari [2, b)] Mario Warran Wizando [3, c)]

[1]*Rubber and Plastic Processing Technology, Politeknik ATK Yogyakarta*
[2,3]*Electrical Engineering, Yogyakarta Respati University*

[a)]Corresponding author:
latifah.listyalina@atk.ac.id
[b)]evrita_lusiana@yahoo.com
[c)]mariowarranw@gmail.com

Abstract. Babies cry based on the discomfort felt by the baby which is a reflex such as when a hungry baby will suck his hand and then he will start crying, hunger can be interpreted from the baby's crying. At each of the baby's cries, when each cryingpattern was responded to with the solution applied to the previous baby, each baby would stop crying. For this reason, to carry out this solution, a research was carried out to identify the pattern recognition of the sound of a baby's cry using the fast fourier transform (FFT) method with several different frequency ranges. The voice recording process is stored in digital form in the form of frequency-based sound spectrum waves, where signals that were previously in the time domain will be changed in the frequency domain. The sounds that will be distinguished in this study include the sounds of crying babies, adults, and colliding objects. This can be obtained through several stages, namely sound sample recording, sampling, signal cutting, frame blocking, final normalization, hamming window, and finally the FFT calculation process. From these series of stages, the results of the frequency range of baby crying are 101-1863 Hz, for adults the frequency range is 101-1376 Hz and for the sound of colliding objects 101-2233 Hz.

INTRODUCTION

The sound of a baby crying is one way of communicating to convey a situation that he experiences when he cries.Babies can make different crying sounds depending on their condition. Baby voice recognition is needed as a quick solution for babies when they cry. In addition, the increase in science and technology is currently developing rapidly.Advances in technology aim to facilitate human activities in all fields, intensive research in the field of signal processing causes technology to develop very rapidly. One of them is speech recognition. [1][2]

Sound is something unique and has a certain frequency range and sound intensity that can and cannot be heard byhumans. The unit for measuring sound intensity is the decibel (dB) taken from the name of its inventor, namely Alexander Graham Bell, who is known as the inventor of the telephone, while the unit for sound frequency is Hertz, taken from the name of a physicist, Heinrich Rudolf Hertz to appreciate services for his contribution in the electromagnetic field. [3][4]. The process of speech recognition by humans begins to form when toddlers are able to hear and are able to make sounds. In this study, the feature extraction of baby crying sound signals was carried out using the Fast Fourier Transform (FFT) method, which is a process of transforming sound signals in the time domaininto frequency signals.

An important process in Digital Signal Processing (DSP) is analyzing an input and output signal to determine thecharacteristics of a particular physical system. The process of analysis and synthesis in the time domain requires a long analysis involving the derivative of the function, which can lead to inaccuracies in the analysis results. Signal

analysis and synthesis will be easier to do in the frequency domain, because the quantity that most determines a signalis frequency. In the time domain, signal analysis cannot be performed. Analysis can be done if the signal is in the formof a spectrum. So it is necessary to transform the signal from the time domain into a frequency domain signal. The function used to view the vibration spectrum of the time domain signal is the Fast Fourier Transform (FFT).

With the above background, in this final project research, a study will be conducted with the title "Implementationof Fast Fourier Transform (FFT) for Baby Cry Detection" because the author sees that babies need special handling in their care. The author wants to make pattern recognition using DFT to generate a frequency spectrum which will then be analyzed by finding the maximum values to determine the frequency range of each sample that has been recorded. If this research can produce data for detecting the sound of a baby crying, this research can be continued tobecome a special nursecall alarm for detecting baby crying, so that it can become a tool that makes it easier for nursesto monitor babies in special baby care rooms.

METHODOLOGY / RESEARCH METHODOLOGY

The research procedures carried out in this study consisted of sampling, sample classification, signal processing, and pattern recognition. The overall research procedure carried out can be seen in the flowchart below.

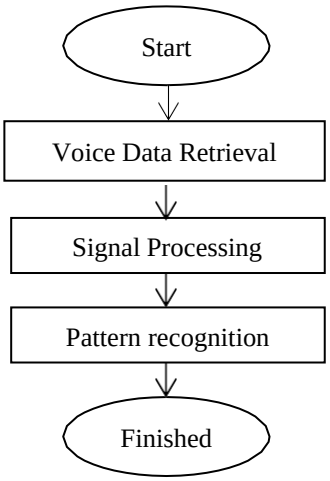

Figure 1. Research Flowchart

Voice Data Retrieval

The sample data is in the form of human voices and the sound of colliding objects. The sound will be used as datain this study. At this stage, the human voice is in the form of a baby crying and the voice of an adult, while the soundof colliding objects is the sound of metal, plastic, wood and glass objects.

The baby sound used is a baby crying from a maternity clinic with a total of ten babies. The adult voice samples used were six adults who were asked to say "My name (name)" and the other four adult voices were noise recordingsand adult chatter. Examples of object impacts are wood knocks, plastic knocks, metal knocks, and glass knocks. Withtwo samples of wood knock, three samples of plastic beat, two samples of metal knock and two samples of glass knock. Voice recording is done using a recording application and then trimming is done so that the audio recording is2 seconds. Then the sound sample will be converted and saved in .wav format. Saved in .wav format because .wav usually uses PCM (Pulse Code Modulation) coding. With this way,

Digital Signal Processing

Signal processing stages are the processes carried out for the process of generating spectrum and FFT. The purposeof this signal processing stage is to equalize the input sound signal so that it is easier to process for speech pattern recognition. The signal processing process has several stages that must be passed, namely normalization, signal cutting, frame blocking, windowing, FFT frequency spectrum, and finding the maximum value of the FFT frequency.The first process is sampling, which is the process of sampling sound waves into a continuous signal. In the process

of sampling there is what is called the sampling rate. The sampling rate indicates how many analog waves are sampledin 1 second. The sampling rate is expressed in Hertz (Hz). The sampling rate used is 44100 Hz. The reason for usinga sampling rate of 44100 Hz is because the limit of the ability of the human ear to perceive sound frequencies is from20 Hz to 20000 Hz, so the most suitable sample rate to use is 44100 Hz. The time used is 2 seconds.

This normalization process is carried out after the output of the sampling process is in the form of wav. In the normalization process, the voice signal must have a maximum value. After searching for the maximum value, the nextstep is to divide the data by the maximum absolute value of the sound recorded.

$$X_{norm} = \frac{x_{in}}{\max\left(abs(x_{in})\right)} \tag{1}$$

where $Xnorm$ is the result of normalized signal data, and Xin is the input data from sampling. The purpose of thisnormalization is to equalize the amplitude of the recorded sound to the maximum, so that the strong or weak effects of the recorded voice do not affect the speech recognition process.

The process of cutting the signal is done to remove the initial signal that is not used and is located on the left sideor the beginning of the signal, namely the silence area and the transition area. The purpose of cutting the silence section is to remove parts that are not part of the sound signal and the research object, and the purpose of cutting the transition area is to get a signal which is the sound signal of the research object. This cutting process is carried out after the normalization process. In the slicing process, the truncated portion is the initial portion of the signal. Signal truncation is done by determining the cutoff limit value, which is 0.3. Then look for the part of the signal that is greaterthan 0.3 and less than -0.3. The searched signal is initialized as b0. The process of cutting the transition area is done by removing ¼ part of the signal that is in the beginning (transition part) after cutting the silence part. Signals that donot include b0 will be omitted, this omitted signal is called the silence signal. Then cutting the transition signal is doneby multiplying the number of signal data by 0.25.

*Frame blocking*is the next process after going through the process of cutting the signal. The value of frame blocking aims to reduce the amount of signal data to be processed. Frame blocking functions to select data from the entire data recorded from the results of signal cutting. The first process carried out in frame blocking is to determine the midpoint value of the sampling data. From the midpoint of the data obtained, it is determined the amount of data to be retrieved for the next process. The value of frame blocking used in this study is 256. The input for the final normalization is the signal from frame blocking. In the frame blocking process, the resulting signal is not optimal, soa final normalization is needed to equalize the amplitude to the maximum. In the final normalization process, The input data resulting from frame blocking is divided by the maximum absolute value of the data resulting from the frame blocking. The result of the division is the output for the final normalization process

*windowing*has a function to eliminate the discontinuity effect caused by the previous process, namely frame blocking when the signal is transformed to the frequency domain. In this study, a hamming window is used where theuse of this window makes the results smoother in eliminating the effects of discontinuities. In this process, the result of frame blocking will be multiplied by the hamming window. This is done to get maximum results in the FFT process,so that samples that have been divided into several frames need to be made into continuous sound.

The process of changing from the time dimension to the frequency dimension begins with finding the computed value of the FFT followed by finding the absolute value of the computed FFT. The process is continued by finding the absolute value of the log value of the results of the FFT mathematical calculation. The computational results are cut by half of the predetermined signal size, then the part to be processed is selected from the results of the cut. The final process in feature extraction is changing the dimensions of the signal. The search for absolute value in each calculation is intended so that the value obtained is a real number so that the calculation process can be continued.

$$X(f) = \int_{-\infty}^{\infty} x(t)\, e^{-i2\pi ft}\, dt$$

$$= \int_{-\infty}^{\infty} x(t)\cos(2\pi ft)\, dt - i\int_{-\infty}^{\infty} x(t)\sin(2\pi ft)\, dt \tag{2}$$

with:
x(t) = function or signal in time domain;
$e-i2\pi ft =$ kernel function;
X(f) = function in the frequency domain
and;f = frequency.
The function of the equation above is used to transform signals from the time domain into the frequency domain.

Pattern recognition

The search process for the maximum value aims to find the maximum values after getting the FFT signal. This process aims to analyze the results of the previous FFT process. These maximum values will be used to determine thepattern of the baby's crying sound. To find the maximum values of the FFT signal, first find the signal data length. Then look for the absolute values of the FFT, and look for the highest values in the FFT signal as an index of the maximum value.

RESULTS AND DISCUSSION

In this study, the human voice is the sound of a baby crying and the voice of an adult, while the sound of colliding objects is the sound of metal, plastic and wood objects colliding. Baby sounds are used with a duration of 2 seconds, but if the recording exceeds 2 seconds, it must be cut using the same application so that the recording becomes 2 seconds. These recordings are still in .mp3 format and must be converted to .wav files so that details are not lost whenthe analog audio is digitized and saved. There were 30 samples in this study, with 10 each for each sample of infants,adults and objects. The sound sampling program uses a sampling frequency of 44100 Hz which is initialized as fs anda duration of 2 seconds which is initialized as t. The following is the result of a plot of one of the recording signals.

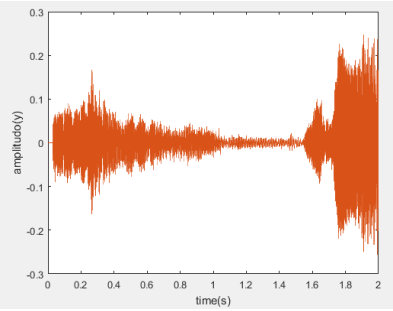

Figure 2. Plot of Sampling Signals (Baby Sounds 1)

In the sampling signal plot above, the x-axis is the recording time of the sound sample and the y-axis is the amplitude of the sound sample, the time is 2 seconds with a maximum amplitude of 0.2473 at 1.911 seconds and a minimum amplitude of -0.2552 at 1.994 seconds.

This normalization process is carried out after the output of the sampling process. In the normalization process, the voice signal must have a maximum value. The reason for using frame blocking 256 is because the higher the frameblocking, the more accurate speech signal recognition will be. Then x1 is the result of normalization, x is the recordedsound signal and max(x) is the maximum value of the recorded sound signal. Normalization is done by dividing the input data (recorded voice signal data) by the maximum value of the data. The following is the result of a plot of oneof the normalized signals

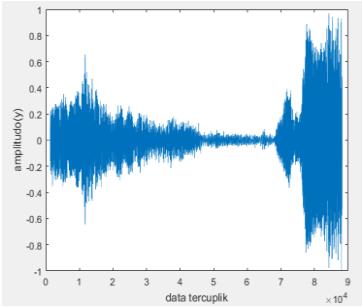

Figure 3. Plotting of Initial Normalized Results (Baby Sounds 1)

In the normalization result plot above, the signal normalization process from the sampling signal or recording signal is carried out in order to equalize the amplitude of the sampling signal data or recording signal so as to obtain the same scale. The x axis is the sampled data and the y axis is the amplitude, the length of the sampled data is 88160and the maximum amplitude is 0.9690 on the sampled data 84260 and the minimum amplitude is -1 on the sampled data 87930.

The next process is cutting the signal which is done twice for the signal from the normalization result. The first cut is made in the silence section or the empty signal section. The second cut is made at the transition. In the silence section signal truncation, data whose height is greater than 0.3 and less than (-0.3) is initialized as b0. Selected >0.3 and <0.3 because these signals are silence signals. Data that does not meet the requirements of b0 is part of the silence signal, so the signal is omitted ([ ]). The following is the result of the signal plot for the silence section.

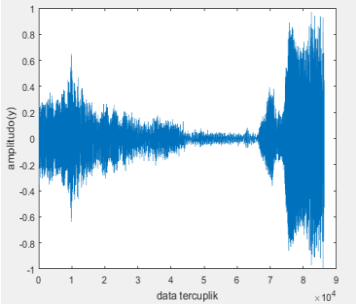

Figure 3. Plotting Results of Intersecting Signal 1 (Baby Sounds 1)

In plotting the results of clipping signal 1 above, the process of removing empty signals in the sense of signals that do not record sound from samples has been carried out. The x-axis is the sampled data and the y-axis is the amplitude, the length of the sampled data is 86300 before the length of the sampled data is 88160, meaning that the length of the sampled data is reduced after cutting this signal. The maximum amplitude is 0.969 in the sampled data 82350 and the minimum amplitude is -1 in the data sampled 86030. This proves that the amplitude remains the same as the amplitude in the previous normalization process, because the normalization process aims to equalize the amplitudes.

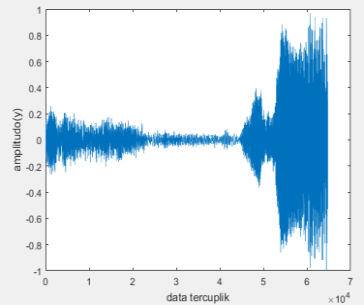

Figure 4. Result of Cutting Signal 2 (Baby Sound 1)

Furthermore, cutting the transition section is carried out by removing ¼ of the signal portion contained in the initial section. The signal is omitted ¼ part of the initial signal in order to obtain a sound signal that is actually recorded. The result of signal cutting 2 above is the process of cutting the transition signal part by cutting ¼ part of the initial signal after cutting the previous silence signal in order to obtain the desired frequency signal. The x axis is the sampled data and the y axis is the amplitude. The length of the sampled data becomes 64720 previously the length of the sampled data was 88160, because 2 transition parts have been cut. The maximum amplitude is 0.969 on the sampled data 60780 and the minimum amplitude is -1 on the sampled data 64490, the amplitude is still the same as the previous signal.

The next process is frame blocking which aims to retrieve some data according to the length of the frame blocking value. The value of frame blocking used is 256 because the higher the frame blocking the speech signal recognition will be more accurate. The retrieved data represents all recorded voice data. x2 is the result of frame blocking. The first process carried out in frame blocking is to determine the midpoint value of the signal clipped data (x1). Then determine the amount of data to be retrieved for the next process. In this process, data is taken starting from the leftmost signal and will be taken along the selected frame value, making it easier to calculate and analyze signals.

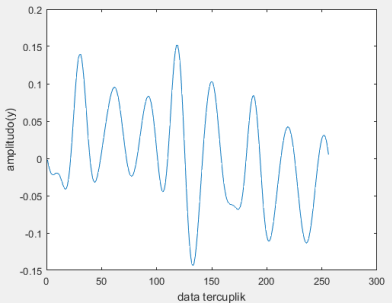

Figure 5. Plotting of Frame Blocking Results (Baby Sounds 1)

The x-axis is the sampled data and the y-axis is the amplitude, the length of the sampled data is 256 before the length of the sampled data is 64720, meaning that the length of the sampled data is reduced after frame blocking is done and this is deliberately done so that the calculation process, signal analysis and recognition of sound patterns become more easy. The maximum amplitude is 0.1517 in the sampled data 119 and the minimum amplitude is -0.144 in the data sampled 133, the frame blocking amplitude is reduced from the previous signal because the signal has been cut according to the length of frame 256 from the leftmost signal.

The final normalization is the normalization after going through the cutting and frame blocking processes. After going through frame blocking, the resulting signal is not optimal, so a final normalization process is needed. The normalization process will be carried out by dividing each data and input value, namely the result of frame blocking with the maximum absolute value of the input data. The purpose of the final normalization is to equalize the resulting frame blocking amplitude so that it is maximized.

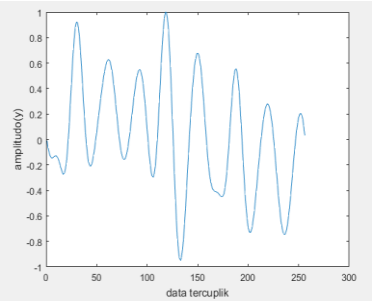

Figure 6. Final Normalized Signal (Baby Sounds 1)

The frame blocking results above are the final normalization process, which is to equalize the amplitude of the frame blocking results so that they are maximized. The x-axis is the sampled data and the y-axis is the amplitude, the length of the sampled data is 256 equal to the length of the previously sampled data in the frame blocking process. The length of the sampled data is the same because in the final normalization process it only aims to equalize the frame blocking amplitude so that it is maximized. The maximum amplitude is 1 in the data sampled 119 and the minimum amplitude is -0.9488 in the data sampled 133. The final normalized amplitude is higher than the previous amplitude because in this process the maximum amplitude value is sought.

hamming window has a function to eliminate the discontinuity effect caused by the previous process, namely frame blocking when the signal is transformed to the frequency domain. So that the sample that has been divided into several frames needs to be made into a continuous sound. This windowing process uses a hamming window. The following is the result of the hamming window.

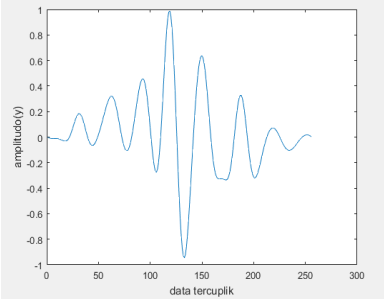

Figure 7. Hamming Window Results (Baby Sounds 1)

The result of the hamming window above is the process of eliminating the discontinuity effect. The x-axis is the sampled data and the y-axis is the amplitude, the length of the sampled data is 256. The maximum amplitude is 0.9875 on 119 sampled data and the minimum amplitude is -0.941 on 133 sampled data.

The next process is the FFT frequency spectrum. The FFT frequency spectrum is a process for obtaining a series of quantities in the recorded signal to determine a learning pattern or test pattern. The FFT calculation aims to find an absolute value which will then be analyzed to determine the pattern of the baby's crying sound.

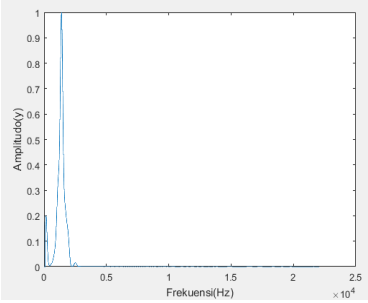

Figure 8. Frequency Spectrum (Baby Sounds 1)

The result of the frequency spectrum above is the final result in knowing the frequency of each sound sample. The x axis is the frequency and the y axis is the amplitude. The following is the frequency data for each sura that has been obtained using frame blocking 256.

Table 1. The Highest Frequency Value of Each Voice

Sample	Highest Frequency (Hz) of Sound		
	Baby	Mature	Object collision
1	1397	139	2233
2	1124	690	1010
3	145	666	226
4	1316	185	286
5	101	163	135
6	786	101	189
7	1863	669	182
8	589	154	101
9	132	1376	120
10	1104	720	258
Highest Frequency Average	**853.9**	**486.3**	**474**
Table Max Value	**1863**	**1376**	**2233**
Table Min Value	**101**	**101**	**101**
Range	**101-1863**	**101-1376**	**101-2233**

From the data obtained above, each frequency has been obtained for each sound sample with frame blocking 256. As the data above, the average infant frequency is 853.9 Hz, the average adult sound frequency is 486.3 Hz, and the average sound frequency object impact 474 Hz. The average frequency of a baby's cry is much higher and has a

significant difference. With higher frame blocking it is easier to see the difference in the average frequency of each sample and finally to recognize patterns of crying babies based on frequency becomes easier.

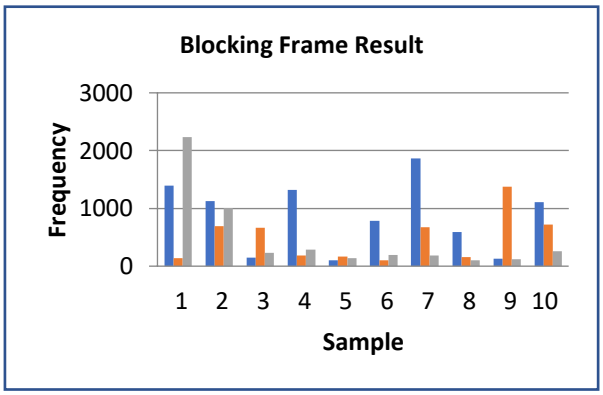

Figure 9. Voice Highest Frequency Data with Frame Blocking 256 (blue for baby, orange for adult, and grey for stuff)

From the data above, it can be concluded that the average frequency of a baby's voice is higher than the frequency of an adult's voice and the sound of colliding objects, so that from that frequency it can be recognized the pattern of the sound of a baby's cry in frequency using the FFT method which was carried out in this study.

CONCLUSION

This chapter contains the conclusions obtained from the identification stage of the recognition of baby crying sound patterns using the fast fourier transform (FFT) method and the conclusions from the frequency range results that have been obtained using the fast fourier transform (FFT) method. So the conclusion is as follows.

The steps for identifying sound signals in pattern recognition of a baby's crying sound are: sound sample recording, sampling, signal cutting, frame blocking, final normalization, hamming window, and finally the FFT calculation process. The frequency range for babies crying is 101-1863 Hz, for adults the frequency range is 101-1376 Hz and for the sound of colliding objects 101-2233 Hz.

REFERENCES

1. MP Brown and K. Austin, The New Physique (Publisher Name, Publisher City, 2005), pp. 25–30.
2. MP Brown and K. Austin, Appl. Phys. Letters 85, 2503–2504 (2004).
3. Fetra, Nicky. 2015. CHORD SEARCH APPLICATION TO ASSIST SONG CREATION USING THE FAST FOURIER TRANSFORM (FFT) ALGORITHM AND K-NEAREST NEIGHBOR (KNN) CLASSIFICATION METHOD. Riau. UIN Sultan Syarif Kasim.
4. Gunawan, D. 2011. DIGITAL SIGNAL PROCESSING WITH MATLAB PROGRAMMING. Jakarta. Science House.
5. Indriani, YH 2015. RECOGNITION OF BELIRA TONE USING AMPLITUDE ANALYSIS IN THE FREQUENCY DREAM. Yogyakarta. Sanata Dharma University.
6. Wahyudi,ST 2015. SPECTRUM ANALYZER APPLICATION TO ANALYZE AUDIO SIGNAL FREQUENCY USING MATLAB. Pekanbaru. Riau University.

ISSN 2745-3502
Volume 4 No. 1 – Agustus 2023
Indonesian Applied Physics Letters

ANDROID APPLICATION FOR EARLY SCREENING OF ATRIAL FIBRILLATION USING DEMPSTER SHAFER METHOD

Rizky Widya Rachmawati[1], Endah Purwanti[2, a)], Marcella Aurelia Yatijan[3], Yudi Her Oktaviono[4], M. Arief Bustomi[5]

[1,2,3] *Biomedical Engineering Study Program, Faculty of Science and Technology, Airlangga University, Campus C, Surabaya 60115, Indonesia*
[4] *SMF Cardiology and Vascular Medicine, Dr Soetomo Hospital, Surabaya 60286, Indonesiaus C, Surabaya 60115, Indonesia*
[5] *Department of Physics, Sepuluh Nopember Institute of Technology, Surabaya, Indonesia*

[a)] Corresponding author: endah-p-1@fst.unair.ac.id

Abstrak. Atrial Fibrillation (FA) is one of the most common heart rhythm disorders found in clinical practice in Indonesia. Atrial fibrillation can cause a 5-fold risk of stroke. Meanwhile, stroke cases tend to increase and become one of the leading causes of death yearly. The cause of high FA cases is the lack of knowledge and public awareness/sensitivity to the early symptoms of the disease. This research aims to design an android device for the initial screening of suspected FA by examining pulse rate, complaints/symptoms and disease risk factors. Dempster Shafer method is used as a decision-making tool for suspected FA or not FA. The detection system performance test results obtained a sensitivity of 93.5%, specificity of 89.7%, and accuracy of 91.7%. The results of the Android application design test, namely Visual Design and User Interaction, Functionality, Stability and Performance and Overall Satisfaction, showed a "good" response in all aspects.

INTRODUCTION

Atrial fibrillation is a heart rhythm disorder (arrhythmia) marked by disorganization of atrial depolarization resulting in disorders of atrial mechanical function (Dinarti et al., 2009). Atrial fibrillation is the most prevalent type of heart rhythm disorder in clinical practice compared to other heart rhythm disorders. According to data from an observational study (MONICA-multinational Monitoring of Trends and Determinants in cardiovascular disease) in an urban population in Jakarta, Indonesia, the prevalence of FA was reported to be 0.2% with a male-to-female ratio of 3:2. The elderly population has a significant increase of 7.74% in 2000-2005, and WHO estimates that it will increase to 28.68% in 2045-2059, so the incidence of atrial fibrillation is also expected to increase significantly. Although this disease is quite common, there is still a lack of knowledge and awareness of FA.

One of the most concerning complications of atrial fibrillation is stroke since patients with atrial fibrillation have a five times higher risk of stroke than those without atrial fibrillation. A FA stroke also results in twice the mortality and a care cost of 1.5 times (Y Yuniadi et al., 2014).

In the health sector, technological advancements have enabled computers to work like experts or doctors, called expert systems. Using an expert system can help find an answer or determine what conclusions can be drawn. An expert system is an artificial intelligence that exists in software built with the ability to approach an expert with high knowledge in a certain area. Hopefully, it can help solve a problem (D Touriano, 2014).

This study aims to design an android application for the initial screening of presumed FA by reading the pulse rate, symptoms, and risk factors. For FA detection, the system uses an artificial intelligence method based on an expert system,

the Dempster-Shafer method. Meanwhile, device evaluation is divided into two schemes: detection performance testing and interface design testing to ensure user comfort. This android application can provide practical knowledge and raise awareness of FA disease to minimize strokes. This will certainly increase work productivity because there is no physical interference/complaint.

Methodology

There are 3 phases carried out in this study: the detection system design phase, the application interface design phase, and the device testing phase. The FA detection system is designed with 19 input parameters (Table. 1) and two outputs (presumed FA or presumed not FA). The classification method used is Dempster Shafer. Data collected in this study used 60 data obtained from interviews and patient medical record data, each consisting of 31 patient data diagnosed with atrial fibrillation and 29 patient data not diagnosed with atrial fibrillation. The criteria used in this study are 19 risk factors and symptoms found in patients with the potential to suffer from atrial fibrillation.

At the knowledge base design phase, parameters are compiled, such as risk factors and symptoms of atrial fibrillation obtained from literature studies, and then discussed with experts, such as cardiologists. After determining the parameters, a process of giving weight or belief values from experts for each parameter is carried out. As shown in Table 1.

TABLE 1. Risk Factor Confidence Score and Atrial Fibrillation Symptoms

Code	Parameter	Belief Value at Risk of Atrial Fibrillation (C1)	Belief Value Not at Risk of Atrial Fibrillation (C2)
G1	The pulse rate felt by the user:	0	0.9
	1. Normal pulse: The pulse has a basic and regular rhythm.		
	2. Abnormal pulse: The pulse has a basic rhythm, but there is a situation of missing one beat between the basic rhythms.	0	0.9
	3. Abnormal pulse rate: The pulse has a basic rhythm, but there is a situation of increasing one beat between the basic rhythms.	0	0.9
	4. Irregular pulse: The pulse has no basic rhythm and is irregular.	0.9	0
G2	Irregular pulse rhythm is caused by physical activity	0.655	0
G3	Rapid heartbeat (Palpitations)	0.9	0
G4	Acute fatigue	0.736	0.164
G5	Shortness of breath (dyspnea)	0.655	0.245
G6	Chest pain or chest pain	0.655	0.327
G7	Dizziness or mild headache	0.736	0.327
G8	Temporary loss of consciousness/fainting (syncope)	0.9	0.164
G9	Active smoker	0.655	0.327
G10	History of Hypertension	0.655	0.164
G11	History of Diabetes Mellitus	0.736	0.327
G12	History of Coronary Heart Disease	0.818	0.164
G13	History of Heart Failure	0.818	0.082
G14	History of Heart Valve Disease	0.9	0.082
G15	History of Stroke	0.818	0.164
G16	History of Chronic Pulmonary Disease	0.9	0.082
G17	Gender:	0.491	0.327
	1. Male		
	2. Female	0.409	0.327
G18	Age ≥ 75 years	0.655	0.327
G19	BMI ≥ 30	0.573	0.327

Second, the application of Dempster Shafer's Theory. Dempster Shafer's theory is representation, combination, and propagation of uncertainty, where this theory has several characteristics that instinctively match the way of thinking of an expert but a strong mathematical basis. In general, Dempster Shafer's theory is written in an interval: [Belief, Plausibility] (Sinaga and Sembiring, 2016). Belief (Bel) measures the evidence's strength in favor of a proposition set. A value of 0 indicates no evidence, and 1 indicates certainty. Plausibility (Pls) will reduce the certainty level of the evidence. Plausibility is 0 to 1. If sure for X', then it can be said that Bel(X') = 1, so the formula above the value of Pls(X) = 0.

There are three steps in the Dempster Shafer method calculation: determining the initial density value (m), the new density value (m), and the largest density value. The initial density value consisting of probabilities of potentially and not potentially suffering from atrial fibrillation is usually called the belief value, and the plausibility value of each parameter is based on the knowledge base. The plausibility value is obtained from the result of 1 - the belief value in the following equation.

$$Pls\ (X) = 1 - Bel\ (X) = 1 - \sum_{Y \subseteq X} m(X)$$

Dimana :
Bel (X) = *Belief* (X)
Pls (X) = *Plausability* (X)
m (X) = *mass function* (X)
m (Y) = *mass function* (Y)

The new density value (m) could be determined by creating a combination table and following the equation below..

$$m3(Z) = \frac{\sum_{X \cap Y=Z} m_1\ (X).m_2(Y)}{1 - \sum_{X \cap Y=\emptyset} m_1\ (X).m_2(Y)}$$

Where:
m3 (Z) = *mass function* from *evidence* (Z)
m1 (X) = *mass function* from *evidence* (X), which is calculated from the belief value of evidence multiplied by the disbelief value of the evidence
m2 (Y) = *mass function* from *evidence* (Y), which is calculated from the belief value of evidence multiplied by the disbelief value of the evidence.
$\sum_{X \cap Y=Z} m_1\ (X).m_2(Y)$ = It is the strength value of evidence Z obtained from the combination of the belief value of a group of evidence.

Detection results are obtained by calculating the Dempster Shafer method with the largest density value. When the density value of C1 is greater than C2, the system will provide detection results of potential atrial fibrillation. It will display the probability value of possible risk factors and symptoms experienced by the user. Still, when the density value of C2 is greater than C1, the system will provide detection results without potentially having atrial fibrillation and display the probability value.

The application interface is designed with three main menus: the info menu to share information about FA and the potential for stroke due to FA, the learning menu to recognize pulse abnormalities, and the detection menu. Furthermore, an expert system test is carried out on the detection results obtained from the calculation of the Dempster Shafer method and then analyzed with three tests, including sensitivity, specificity, and accuracy.

The sensitivity value is used to see the likelihood of patients potentially affected by atrial fibrillation from the overall data of patients with the potential to have atrial fibrillation. The sensitivity value is obtained by matching the results of expert diagnosis on patients diagnosed with atrial fibrillation with the calculation results of the method used as the conclusion of the system output. This value also determines how well the method predicts the potential for atrial fibrillation. The calculation to determine the sensitivity value can be done using the following equation.

$$\text{Sensitivitas} = \frac{TP}{TP+FN} \text{ x } 100\%$$

Keterangan:
TP = *True Positive*
FN = *False Negative*

True Positive is a result where the Dempster-Shafer method correctly predicts data potentially having atrial fibrillation. False Negative is a result where the Dempster Shafer method incorrectly predicts data potentially having atrial fibrillation.

The specificity value is used to see the possibility of patients who do not have the potential to have atrial fibrillation from all patient data that does not have the potential to have atrial fibrillation. The specificity value is obtained by matching the expert diagnosis results in patients not diagnosed with atrial fibrillation with the calculation results of the

method used as the conclusion of the system output. This value is also used to determine how well the method is used in predicting not potentially having atrial fibrillation. The calculation to determine the sensitivity value can be done using the following equation.

$$\text{Specificity} = \frac{TN}{TN+FP} \text{ x } 100\%$$

Keterangan:
TN = *True Negative*
FP = *False Potitive*

True Negative is a result where the Dempster-Shafer method correctly predicts data that does not have the potential to have atrial fibrillation. False Positive is a result where the Dempster Shafer method incorrectly predicts data that does not have the potential to have atrial fibrillation.

The accuracy value is used to measure the accuracy of atrial fibrillation prediction by comparing the results of expert diagnosis. This value is obtained by using all the prediction results from the method used and compared with the results of the expert diagnosis. The higher the accuracy value, the more precise the method is in predicting the potential for atrial fibrillation. The calculation to determine the accuracy value can use the following equation..

$$Accuracy = \frac{\sum true\ data}{N} . 100\ \%$$

Keterangan :
∑ true data = Total number of matching data between expert diagnosis results and system output results
N = The number of trials conducted

In this study, the expert system used is implemented into an Android-based application so that an application test is needed, which aims to find out whether the application is good enough or not and eliminate any bugs and errors in the application that has been made. It is intended that the application can be used easily by all users.

According to Google Play Developer Guidelines, two tests must be carried out in an Android program: User Satisfaction Test and Software Testing. The User Satisfaction Test aims to determine the level of user satisfaction with the application that has been made. The application will be submitted to the user for testing and survey in this test. This test can also be used as a means of finding bugs and asking for suggestions so that the application can be better. Testing is done using a questionnaire that includes important aspects. Important aspects of the satisfaction test in Nuzul (2016) include ease of user interface, functionality, stability, performance, and overall satisfaction with a rating scale of 1-10.

Software Testing aims to perfect the application that has been made. Software testing methods are divided into two, namely, White Box Testing and Black Box Testing. White Box Testing is a testing method by looking at the program listing to examine the program code, which is then analyzed for errors and whether the desired output is appropriate or not based on the program code that has been created. At the same time, Black Box Testing is a method carried out by analyzing whether the application output follows the desired process and results. This test method sees whether the final result of the application process is built following the initial design of making the application, both in terms of functionality and internal structure.

RESULT AND DISCUSSION

This study used 60 patient data at Universitas Airlangga Hospital, with details of 31 patients diagnosed with atrial fibrillation and 29 patients not diagnosed with atrial fibrillation. After the parameters selected by the user are entered, and the system calculates the Dempster Shafer method, the results of the expert system prediction of the Dempster Shafer method are matched with the results of the expert diagnosis, as shown in Table 2.

\

TABEL 2. Matching System Prediction Results with Expert Diagnosis

Data to-	Expert Diagnoses	*System Outputs*	Description
1	Potential to have Atrial Fibrillation	Potential to have Atrial Fibrillation	Conforming
2	Potential to have Atrial Fibrillation	Potential to have Atrial Fibrillation	Conforming
3	Potential to have Atrial Fibrillation	Potential to have Atrial Fibrillation	Conforming
4	Potential to have Atrial Fibrillation	Potential to have Atrial Fibrillation	Conforming
5	Potential to have Atrial Fibrillation	No Potential to have Atrial Fibrillation	non-conforming
6	Potential to have Atrial Fibrillation	Potential to have Atrial Fibrillation	Conforming
7	Potential to have Atrial Fibrillation	Potential to have Atrial Fibrillation	Conforming
8	Potential to have Atrial Fibrillation	Potential to have Atrial Fibrillation	Conforming
9	Potential to have Atrial Fibrillation	Potential to have Atrial Fibrillation	Conforming
10	Potential to have Atrial Fibrillation	Potential to have Atrial Fibrillation	Conforming
11	Potential to have Atrial Fibrillation	Potential to have Atrial Fibrillation	Conforming
12	Potential to have Atrial Fibrillation	Potential to have Atrial Fibrillation	Conforming
13	Potential to have Atrial Fibrillation	Potential to have Atrial Fibrillation	Conforming
14	Potential to have Atrial Fibrillation	Potential to have Atrial Fibrillation	Conforming
15	Potential to have Atrial Fibrillation	Potential to have Atrial Fibrillation	Conforming
16	Potential to have Atrial Fibrillation	Potential to have Atrial Fibrillation	Conforming
17	Potential to have Atrial Fibrillation	Potential to have Atrial Fibrillation	Conforming
18	Potential to have Atrial Fibrillation	Potential to have Atrial Fibrillation	Conforming
19	Potential to have Atrial Fibrillation	Potential to have Atrial Fibrillation	Conforming
20	Potential to have Atrial Fibrillation	Potential to have Atrial Fibrillation	Conforming
21	Potential to have Atrial Fibrillation	Potential to have Atrial Fibrillation	Conforming
22	Potential to have Atrial Fibrillation	Potential to have Atrial Fibrillation	Conforming
23	Potential to have Atrial Fibrillation	Potential to have Atrial Fibrillation	Conforming
24	Potential to have Atrial Fibrillation	Potential to have Atrial Fibrillation	Conforming
25	Potential to have Atrial Fibrillation	Potential to have Atrial Fibrillation	Conforming
26	Potential to have Atrial Fibrillation	Potential to have Atrial Fibrillation	Conforming
27	Potential to have Atrial Fibrillation	Potential to have Atrial Fibrillation	Conforming
28	Potential to have Atrial Fibrillation	No Potential to have Atrial Fibrillation	non-conforming
29	Potential to have Atrial Fibrillation	Potential to have Atrial Fibrillation	Conforming
30	Potential to have Atrial Fibrillation	Potential to have Atrial Fibrillation	Conforming
31	Potential to have Atrial Fibrillation	Potential to have Atrial Fibrillation	Conforming
32	No Potential to have Atrial Fibrillation	No Potential to have Atrial Fibrillation	Conforming
33	No Potential to have Atrial Fibrillation	No Potential to have Atrial Fibrillation	Conforming
34	No Potential to have Atrial Fibrillation	No Potential to have Atrial Fibrillation	Conforming
35	No Potential to have Atrial Fibrillation	No Potential to have Atrial Fibrillation	Conforming
36	No Potential to have Atrial Fibrillation	No Potential to have Atrial Fibrillation	non-conforming
37	No Potential to have Atrial Fibrillation	No Potential to have Atrial Fibrillation	Conforming
38	No Potential to have Atrial Fibrillation	No Potential to have Atrial Fibrillation	Conforming
39	No Potential to have Atrial Fibrillation	No Potential to have Atrial Fibrillation	Conforming
40	No Potential to have Atrial Fibrillation	Potential to have Atrial Fibrillation	non-conforming
41	No Potential to have Atrial Fibrillation	No Potential to have Atrial Fibrillation	Conforming
42	No Potential to have Atrial Fibrillation	No Potential to have Atrial Fibrillation	Conforming
43	No Potential to have Atrial Fibrillation	No Potential to have Atrial Fibrillation	Conforming
44	No Potential to have Atrial Fibrillation	No Potential to have Atrial Fibrillation	Conforming
45	No Potential to have Atrial Fibrillation	No Potential to have Atrial Fibrillation	Conforming
46	No Potential to have Atrial Fibrillation	No Potential to have Atrial Fibrillation	Conforming
47	No Potential to have Atrial Fibrillation	No Potential to have Atrial Fibrillation	Conforming
48	No Potential to have Atrial Fibrillation	No Potential to have Atrial Fibrillation	Conforming
49	No Potential to have Atrial Fibrillation	No Potential to have Atrial Fibrillation	Conforming
50	No Potential to have Atrial Fibrillation	No Potential to have Atrial Fibrillation	Conforming
51	No Potential to have Atrial Fibrillation	No Potential to have Atrial Fibrillation	Conforming
52	No Potential to have Atrial Fibrillation	Potential to have Atrial Fibrillation	non-conforming
53	No Potential to have Atrial Fibrillation	No Potential to have Atrial Fibrillation	Conforming
54	No Potential to have Atrial Fibrillation	No Potential to have Atrial Fibrillation	Conforming
55	No Potential to have Atrial Fibrillation	No Potential to have Atrial Fibrillation	Conforming
56	No Potential to have Atrial Fibrillation	No Potential to have Atrial Fibrillation	Conforming
57	No Potential to have Atrial Fibrillation	No Potential to have Atrial Fibrillation	Conforming
58	No Potential to have Atrial Fibrillation	No Potential to have Atrial Fibrillation	Conforming
59	No Potential to have Atrial Fibrillation	No Potential to have Atrial Fibrillation	Conforming
60	No Potential to have Atrial Fibrillation	No Potential to have Atrial Fibrillation	Conforming

Determination of the performance of the Dempster Shafer method can be determined by three testing methods,

namely sensitivity, specificity, and accuracy.

From the tests carried out according to Table 2, the number of true positive (TP) data is 29, and false negative (FN) data is 2. So that the sensitivity value of the Dempster-Shafer method in predicting the potential for atrial fibrillation is 93.7%. While the true negative (TN) is 26 data and the false positive (FP) is three, the specificity value of the Dempster-Shafer method in predicting the absence of the potential for atrial fibrillation is 89.7%. So that the accuracy of the Dempster-Shafer method in predicting the presence and absence of the potential to have atrial fibrillation is 91.7%.

The expert system in this research is implemented into an Android-based application. Interface design provides an overview of the application display that the user will use. The results of the interface design in this study consist of the main, learning, detection, info, and help windows.

The main display window is the initial display in a splash screen, and the main menu is shown in Figure 1. In the main menu, there are four menus, namely the learning menu, detection menu, info menu, and help menu.

The learning menu contains a video of how to feel the pulse because, in this study, the main parameter used is the pulse condition; it is necessary to learn in advance about how to handle the pulse and recognize various pulse conditions. The display of the learning menu is shown in Figure 2.

According to the knowledge base, the detection menu contains questions in the form of symptoms and risk factors for atrial fibrillation. On the initial page of the detection menu, the user will be presented with a video in the form of 4 pulse conditions (Figure 3). The first video is a description of a normal pulse condition, namely a pulse that has a primary and regular rhythm, the second is a description of a pulse condition that has a basic rhythm, but there is a loss of one beat between primary rhythms, The third is a description of the condition of the pulse having a basic rhythm but there is a state of increasing one beat between the primary rhythms, and the fourth is a description of the condition of the pulse not having a basic and irregular rhythm, the fourth pulse state is a description of the pulse state experienced by atrial fibrillation patients. Then the user chooses one of the pulse videos that best suits their feelings. Furthermore, the user will answer questions about symptoms and risk factors for atrial fibrillation by answering yes or no, choosing a history of illness experienced, and filling in height, weight and age, as shown in Figure 4. At the end of the question, there will be a detection button; Figure 5 is an example of the conclusion of the detection results generated by the application.

The Info menu is shown in Figure 6; in the info menu, there are three menus; the first is the atrial fibrillation information menu; this menu contains an understanding of potential dangers due to atrial fibrillation and symptoms and risk factors for atrial fibrillation. The second menu is the application information menu; this menu contains information about the application's purpose and the application's test results. The third menu is the programmer information menu; this menu includes information from the application creator.

The Help menu contains procedures for running the application, so it is expected to help users use it. The display of the help menu is shown in Figure 7.

(a) (b)

FIGURE 1. Main Window (a) Initial View (b) Main View

FIGURE 2. Learning Menu

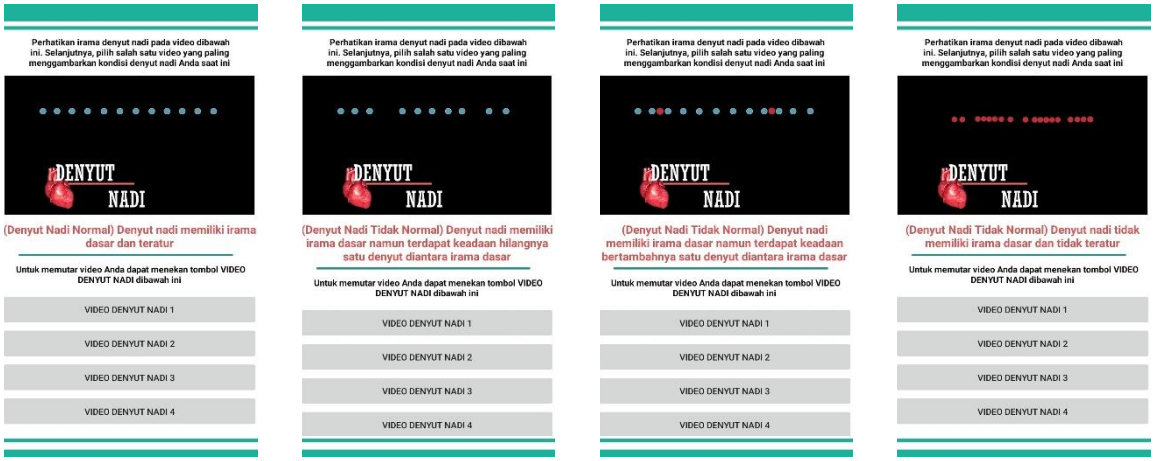

FIGURE 3. Pulse condition detection menu (a) Normal pulse, (b) Pulse with one beat missing at basic rhythm, (c) Pulse with one beat added at basic rhythm, (d) Irregular pulse and no basic rhythm.

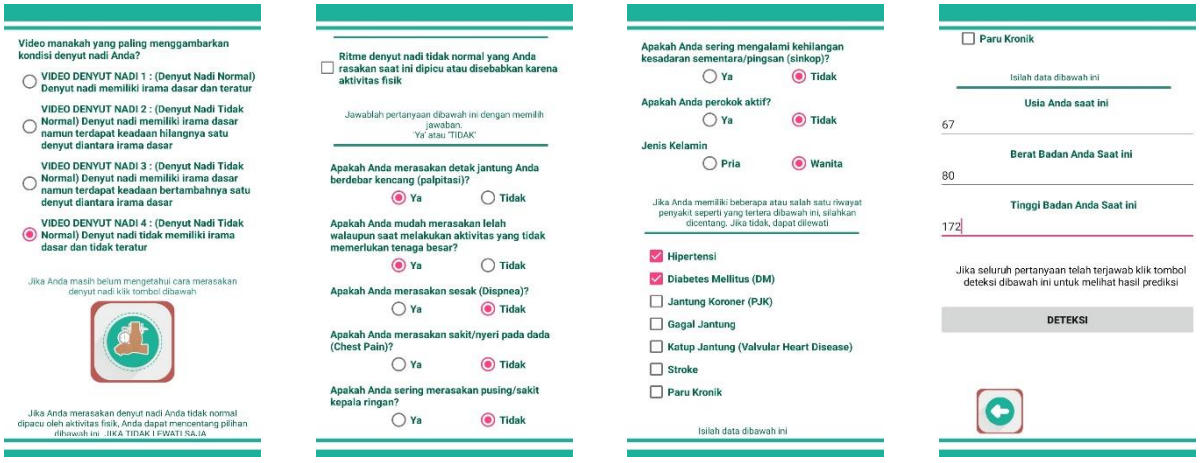

FIGURE 4. Detection menu (a) Menu matching pulse rate with video, (b) Detection with history, (c) Disease history, (d) Patient data

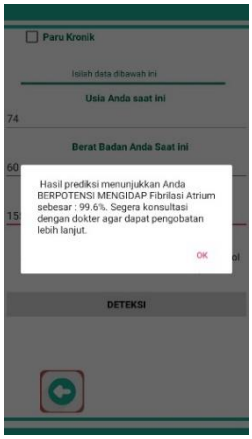

FIGURE 5. Detection Results

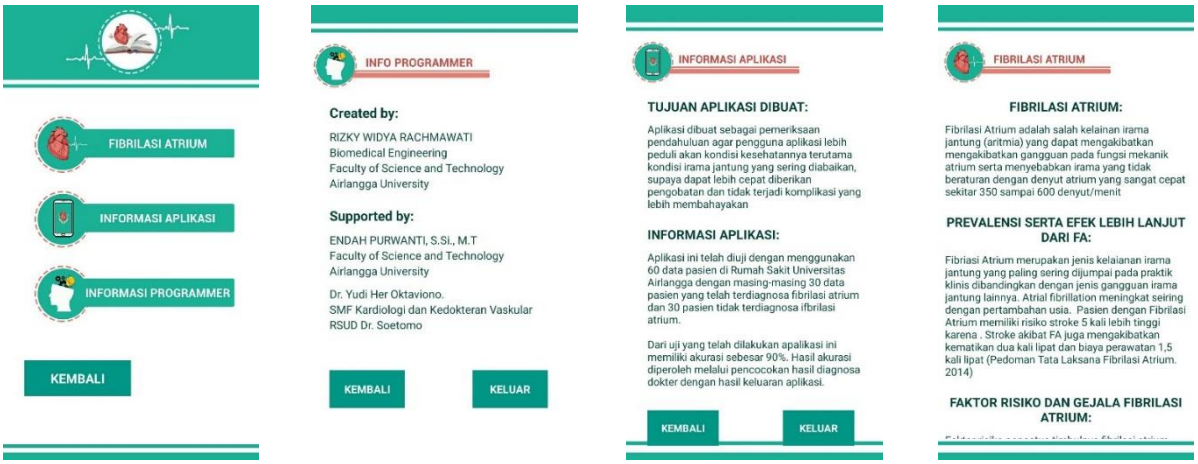

(a) (b) (c) (d)

FIGURE 6. Info menu (a) Info menu list, (b) Programmer info, (c) Application Information, (d) Atrial Fibrillation

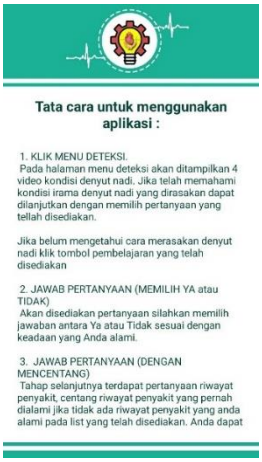

FIGURE 7. The Help menu

Next, the User Satisfaction Test. In this test, the atrial fibrillation detection application is handed over to the user to try and then test and survey user satisfaction when using the application. The test was carried out by filling out a questionnaire conducted by 20 randomly selected people, and then the average value of the assessment results was calculated. This test has essential aspects, namely visual design and user interaction, functionality, stability, performance, and overall satisfaction, with a rating scale of 1-10. The number 1 indicates very bad, cannot function, and has errors. While the number 10 shows very good, can function properly and has no errors. The test results of the user satisfaction test can be seen in Table 3 to Table 6.

TABLE 3. Survey Results of Visual Design and Program User Interaction

No	Subject	Average Value
1	Icon display on the Android menu screen	8,4
2	Initial splash screen display	8,4
3	Detection window display	8,1
4	Learning window display	8
5	Info window display	8,1
6	Help window display	7,9
7	Ease of finding the Detection icon on the main menu screen	8,7
8	Ease of doing the parameter filling process in the detection window	8
9	Ease of displaying detection results	8,4
10	Ease of returning to the main page of the application	8,4
11	The level of convenience and appearance of the application as a whole	8,3

The average value obtained from the survey results is above 8 in visual design and user interaction. But only the appearance of the help window only got a value of 7.9. In visual design and user interaction, it is expected that the application has been made has met the standards of the Android Design Guidelines. These standards include the use of the icon system should not deviate far from the function of the application, support the back button feature and so on.

TABLE 4. Program Functionality Survey Results

No	Subject	Average Value
1	Response to the opening of the atrial fibrillation detection application when you press the icon on the menu screen	8,8
2	The learning button on the main page can function properly	8,9
3	The detection button on the main page can function properly	9
4	The info button on the main page works well	9
5	The help button on the main page works well	8,9
6	The atrial fibrillation information button on the info page works well	8,9
7	The application information button on the info page works well	8,9
8	The programmer information button on the info page works well	8,7
9	The detection process runs properly	8,7
10	Ease of understanding the contents of the learning window	8,2
11	Ease of understanding the contents of the atrial fibrillation info window	8,2
12	Ease of understanding the contents of the programmer info window	8,2
13	Ease of understanding the contents of the application info window	8,2
14	Ease of understanding the contents of the help window	8,4
15	Ease of understanding the detection results provided	8,5
16	The learning button on the detection window can function properly	8,7
17	The video play button on the detection window can function properly	8,8
18	The video play button on the learning window can function properly	8,9
19	The next button on the learning window can function properly	8,9
20	The exit button on the main page can function properly	8,9
21	The level of functionality of the components contained in the application	8,7

The average value obtained from the survey results is above 8 in program functionality. In program functionality, it is expected that the application that has been made can at least run and function properly and correctly on the targeted device.

TABLE 5. Stability and Performance Survey Results

No	Subject	Average Value
1	No lag, crash, force close, freeze when running the application	8,1
2	The response rate of application usage	8,2
3	No errors during the detection process	8,2
4	Application performance and stability level	8,5

The average value obtained from the survey results is above 8 in the stability and performance program. In the stability and performance program, it is expected that the application that has been made is at least able to run and function properly and correctly on the targeted device.

TABLE 6. Overall Satisfaction Testing Results

No	Subject	Average Value
1	Your assessment when using the app	8.5
2	Level of ease when performing the pulse learning process on the application	8.6
3	Level of ease when performing the detection process	8.6
4	The level of benefit from using the application	8.7
5	How much do you want the development of the atrial fibrillation detection application to continue	9,4

In overall satisfaction, the average value obtained from the survey results is above 8. In overall satisfaction, it is expected to know the general level of satisfaction with the application that has been made.

TABLE 7. Overall Average of Survey Results

No	Subject	Average Value
1	Visual Design and User Interaction	8,2
2	Functionality	8,7
3	Stability and Performance	8,3
4	Overall Satisfaction	8,7

Table 7 shows that the average value of the aspects surveyed to 20 randomly selected users is above 8. In Visual Design and User Interaction, the average value is 8.2. This shows the level of user satisfaction with the design and interaction of the application is quite good. On functionality, an average value of 8.7 is obtained. This shows that the application that has been made can function correctly. On stability and performance, an average value of 8.3 is obtained. This indicates that the application can run well with minimal potential for interference, such as lag, force close, errors, and so on. In overall satisfaction, an average value of 8.7 is obtained. This shows that the level of user satisfaction is relatively high overall in the application that has been made.

The software testing results with the White Box Texting testing method are carried out by looking at the program listing to examine each program code and analyze whether or not there are errors and whether the desired output follows the program code that has been made. The Black Box Testing method is done by running the application and then analyzing whether the final result of the application process is built following the initial design of making the application or not. The results of testing the application with the Black Box Texting method can be seen in Table 8

TABLE 8. Application Testing Results with Black Box Texting Method

No	Testing Procedure	Expected Output
1	Click the application icon	Display Splashscreen
2	Click the learning menu button	Display the learning page
3	Click the detection menu button	Displays a page containing questions to detect atrial fibrillation
4	Click the info menu button	Displays a page containing three options in the form of info buttons, including Atrial fibrillation info, application info, and programmer info
5	Click the atrial fibrillation info menu button	Displays a page containing information about atrial fibrillation
6	Click the application info menu button	Displays a page containing information about the application
7	Click the programmer info menu button	Displays a page containing information about the programmer
8	Click the help menu button	Displays a page containing help on how to use the application
9	Click pulse video button 1	Plays pulse video 1
10	Click the pulse video button 2	Playing the pulse video 2
11	Click the pulse video button 3	Playing the pulse video 3
12	Click the pulse video button 4	Playing the pulse video 4
13	Click the "Yes" or "No" Radiobutton	You can choose one of the answers by pressing the "Yes" or "No" button
14	Click the checkbox or not	You can choose by pressing or not pressing the checkbox following the selected parameters
15	Filling Edit Text	You can fill in the edit text field
16	Click the detection button	Displays detection output along with probability value and suggestions.
17	Click the back button	Displays the previous page
18	Click the Continue button	Displays the next page
19	Click the exit button	Displays a question to close the application
20	Click the "Yes" button on the exit menu	Close the application
21	Click the "No" button on the exit menu	Does not close the application

From the results of Black Box Testing in Table 5. This shows that the expert system application designed in this study can run well according to its functions.

CONCLUSIONS

Atrial fibrillation detection application as an effort to reduce the potential for stroke with the Dempster Shafer method has been successfully developed. The application is made with android-based and can detect the presence or absence of the potential to have atrial fibrillation based on 19 parameters in the form of risk factors and symptoms of atrial fibrillation. From the test results that have been carried out in this study using 60 test data consisting of 31 patient data that has been diagnosed with atrial fibrillation and 29 patients who were not diagnosed with atrial fibrillation, the sensitivity, specificity, and accuracy values of the Dempster Shafer method are 93.5%, 89.7%, and 91.7%.

REFERENCES

1. Alan S. et al .2001. Prevalence of diagnosed atrial fibrillation in adults. American Medical Association.
2. Aliferi Chryssa. 2016. Android Programming Cookbook. Java Code Geeks.

3. Chern, et al. 2012. Distribution and Risk Profile of Paroxysmal, Persistent, and Permanent Atrial Fibrillation in Routine Clinical Practice Insight from the Real-Life Global Survey Evaluating Patients With Atrial Fibrillation International Registry. Aha Journal.
4. Dinarti Lucia K, Suciadi Leonardo P. 2009. Stratifikasi Risiko dan Strategi Manajemen Pasien dengan Fibrilasi Atrium. Maj Kedokteran Indonesia, Volum:59, Nomor:6, Juni 2009.
5. Farosi, K., Nuryani, dan Darmanto.2017. Optimasi Fuzzy Inference System pada Sistem Deteksi Fibrilasi Atrium dengan Fitur Elektrokardiogram. Jurusan Fisika, Fakultas Matematika dan Ilmu Pengetahuan Alam, Universitas Sebelas Maret.
6. Imam Syafi'i, et al. 2014. Rancang Bangun Sistem Pakar Diagnosis Gangguan Preferensi Seksual Menggunakan Metode Certainty Factor Pada Institusi Kepolisian. Jurnal Sistem Informasi, Volume. 3, Nomor.2 (2014).
7. Indraswari, D.P., Soebroto, A.A., dan Marharndraputro, E.A. 2015. Sistem Pendukung Keputusan Deteksi Dini Penyakit Stroke Menggunakan Metode Dempster- Shafer. Program Teknologi Informasi dan Ilmu Komputer, Universitas Brawijaya.
8. Melvin M. Scheinman. Atrial Fibrillation. MD. by McGraw-Hill/Appleton & Lange, 2002. Second Edition. Current Diagnosis & Treatment in Cardiology D Touriano, dkk. 2014. Sistem Pakar Mendiagnosa Penyakit Jantung Dengan Metode Fuzzy Set. Universitas Islam Indonesia.
9. Rahardian, T. 2018. Rancang Bangun Aplikasi Deteksi Infark Miokard Akut Dengan Metode Dempster Shafer Berbasis Android. Surabaya. Teknik Biomedis, Fakultas Sains dan Teknologi, Universitas Airlangga.
10. Y Yuniadi, Tondas AE, Hanafi DA, dkk. 2014.Pedoman Tata Laksana Fibrilasi Atrium Edisi Ketiga. Centra Communications.
11. Sinaga, M. D dan Sembiring, N. S. Br. 2016. Penerapan Metode Dempster Shafer untuk Mendiagnosa Penyakit dari Akibat Bakteri Salmonella. Cogito Smart Journal/Vol. 2/No.2
12. Wolf P. A., et al. 1991. Atrial Fibrillation as an Independent Risk Factor for Stroke: The Framingham Study. Journal of American Heart Study.

ISSN 2745-3502
Volume 4 No. 1 – Agustus 2023 *Indonesian Applied Physics Letters*

On the Design of Maze Wanderer Robot

Mohanad Abdulhamid[1,a)]

[1] Al-Hikma University, Iraq

[a)] moh1hamid@yahoo.com

Abstract. This paper focuses on designing, programming and implementing a maze wonderer robot that takes the commands to dictate its direction of motion based on the obstacle avoidance. A program is to be written to give the robot its intelligence. The paper will as well be restricted to a motorized car which will be given the intelligence to be able to navigate through a given maze.

INTRODUCTION

Robots are intelligent machines capable of doing tasks they are programmed to do. They have shown significance in decreasing human work load especially in industries. If there is one technological advancement that would certainly make living easy and convenient, robots would be the answer.

Robots are mostly utilized in the manufacturing industry. People who do the same thing for a long period of time tend to get bored and tired of what they are doing and might arrive in a position wherein they are unwillingly doing their job. The person who reached this point will not be as efficient and effective as when they first started working. Also, as human beings, we get exhausted so the length of time that we can work is limited. This is when the importance of robots is realized. They can be set to function for a long span of time producing the same quality product all throughout the production process. This results to an increase in the number of manufactured products of consistent quality and decrease in the production of defective goods.

Industries can gain a lot of benefits out of robotics. The company productivity will rise making businesses achieve more profits. Also, company losses will be reduced because flawed products are trimmed down to almost none. The importance of automation and robotics in all manufacturing industries is growing. Robots can replace human beings in a wide variety of industries. Robots outperform humans in jobs that require precision, speed, endurance and reliability. Robots safely perform dirty and dangerous jobs. Robots need no environmental comforts as compared to humans and can process multiple tasks simultaneously.

For repetitive tasks which use the same path in a factory to remove the need for a human operator, path can be used as a guide for a robot lawnmower. Smarter versions of path followers can be used to deliver mail within an office building and deliver medications in a hospital. The technology has been suggested for running mass transit systems within a factory/industry and may end up as part of autonomous cars navigating the freeway.

Rescue robots in development are being made with abilities such as searching, reconnaissance and mapping, removing rubble, delivery of supplies such as medical supplies or even evacuations of casualties.

From the above uses one can be convinced that indeed a robot is a very important device in our day-to-day operations. Thus, proper design and implementation of this instrument, taking into consideration safety, accuracy and precision, cost and efficiency has been an engineering concern to meet the ever growing demand of the device. Some works on the topic of robot design can be found in literatures[1-6].

IMPLEMENTATION METHODOLOGY

Hardware development

The hardware part must be correctly design to ensure that the operation will work appropriately as desired. The main operation is to define how to control the DC motors using the H-bridge and the sensor and how to connect this combined circuit to the micro-controller circuit. The H- bridge and the micro-controller are being controlled by the micro-controller

program code.

The main circuit consists of a combination of three circuits; the power supply unit, sensory array module, central processing unit (controller) and the drive system which is the motor control unit, all are discussed in the next sections.

Central processing unit (controller)

Control unit refers to an electronic system which takes inputs from the various sensors which collect data from the environment and can drive the output devices according to the conditions which are applied due to various constraints. The control unit consists of a programmable logic device called microcontroller. The microcontroller is a type of electronic device which can be pre-programmed according to our requirements. Every microcontroller has various input and output pins where different I/O devices can be connected. The microcontroller also has other peripherals embedded inside the same chip. Therefore microcontroller is nothing but a microprocessor with all other peripherals embedded inside the same chip. Whenever we have to control the systems dynamically according to the conditions of system environment, we use a microcontroller as the control unit.

Design of the obstacle sensing unit

Each infrared range sensor measures the distance to an object by detecting reflected infrared light transmitted by its light emitter. This is illustrated in Fig.1. The electronics in the sensor enable it to measure the angle at which the reflected light enters the detector. When the sensor is close to an object, light enters the detector at a sharp angle. When the sensor is far from an object, light enters the detector at a slight angle. The sensor outputs an analog voltage that varies depending on the angle at which the reflected light enters the detector. This technique makes the sensor insensitive to ambient light and the reflectivity of the detected object, ensuring the output voltage is solely a function of the distance to the detected object.

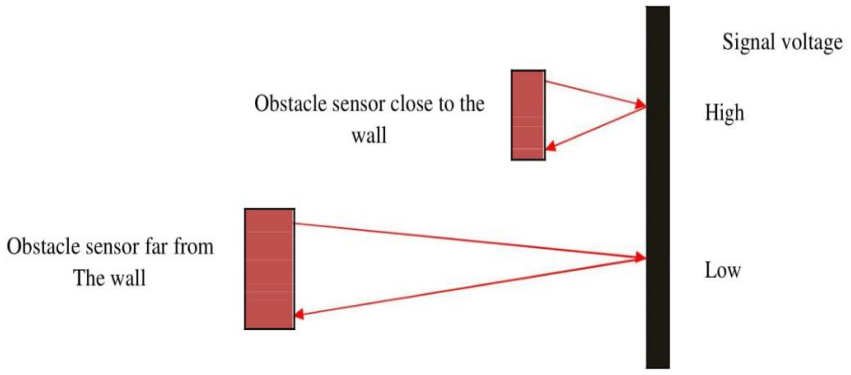

FIGURE 1. Sensing Distance to the Obstacle

The infrared based object detector can be implemented using two configurations; break beam sensors and reflectance sensors. The second configuration is very suitable for the portability of this robot where both the infrared(IR) source and the IR detector need to be on the robot; hence it is going to be implemented in the control system of the robot. The infrared emitter-detector basic circuit is as shown in Fig.2.

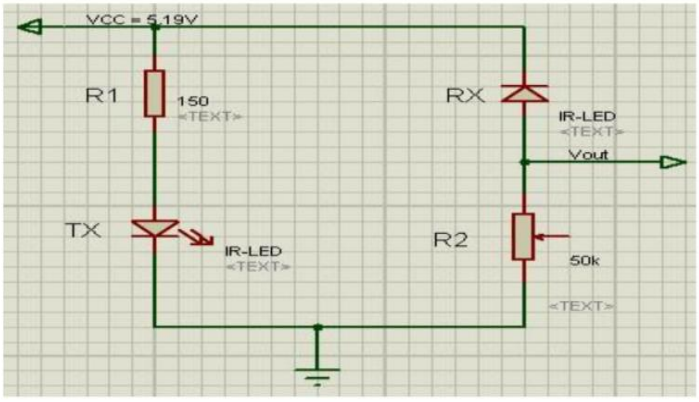

FIGURE 2. Infrared emitter-detector basic circuit

R1 is chosen to be 220Ω to prevent the light emitting diode(LED) from melting itself. The resistance value of R2 determines the sensitivity of the robot in terms of the distance between the robot and the obstacle. For R1 = 220Ω, R2 = 22KΩ and Vcc = 5.19V, if no obstacle is in front of the sensor then the value of Vout is around 2.05V and when an obstacle comes to about 15cm from it, the value goes up to 3.78V, and when the obstacle comes nearer than 5cm the value saturates to 5.06V.

Similarly, six units of the obstacle detector circuits designed above are going to be used, two for detecting left wall obstacles during the forward motion, two for detecting front obstacles and turning right if there is an obstacle in front. One on the right to determine when to move forward when there a reverse initially and one on the rear part in order to turn when reversing.

All the outputs from the sensors are analogue in nature and since the microcontroller to be used has only six pins that can do analogue to digital conversion. In addition to the microcontroller that is going to do the analogue to digital conversion, it also performs the signal processing.

Design of the control signals processing unit

Output signals from the obstacle detection unit are used as inputs to the control signals processing unit. These include the six inputs from the other six inputs from the obstacle detector circuits. Hence the control signals processing unit will have six inputs from the obstacle detection unit which are all digital in nature.

Since the input signals are analogue signals, the first step is to convert them to digital signals using the analogue to digital conversion feature of the microcontroller. Next step is to perform logical operations on the digital signals; for the obstacle detection circuits, the one with the highest value (meaning receiving the highest value due to complete obstability) is determined to indicate the direction of motion of the robot and for the obstacle sensors, their values are used to determine whether the motion to a given direction can be permitted.

The robot will have a total of six IR sensors, all oriented strategically to determine the motion of the robot. Orientation of the sensors is as shown in Fig.3.

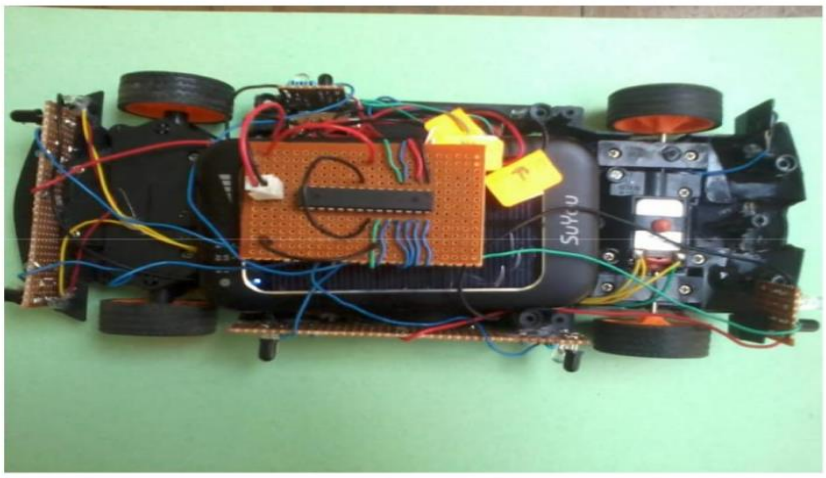

FIGURE 3. Orientation of the IR infrared sensors

The total number of sensors that the robot is expected to use are six. This implies that there will be a number of combinations as the various sensors will be giving different readings at any instant of time.

Software development

The primary purpose of the software is to maintain control over the hardware at all times and determine where to move by solving the maze. Controlling the hardware consist of reading the sensors; setting the motor speed and communicating with any external peripherals

Algorithm

The principal goal of a robot is to solve the maze and find its end. To accomplish this task, the robot uses a particular maze searching algorithm. A vast amount of research on searching techniques already exists and is currently being

undertaken. As a result, robots generally use some variation of the following three searching algorithms: wall follower, depth first search and flood fill. Only, wall follower algorithm is considered here.

Wall follower algorithm

The wall follower, the best-known rule for traversing mazes, is also known as either the left-hand rule or the right-hand rule. If the maze is simply connected, that is, all its walls are connected together or to the maze's outer boundary, then by keeping one hand in contact with one wall of the maze, the robot is guaranteed not to get lost and will reach a different exit; otherwise, the robot will return to the entrance having traversed every corridor in the maze at least once.

Another perspective into why wall following works, is topological. If the walls are connected, then they may be deformed into a loop or circle. Then wall following reduces to walking around a circle from start to finish. To further this idea, by grouping together connected components of the maze walls, the boundaries between these are precisely the solutions, even if there is more than one solution.

If the maze is not simply connected (if the start or endpoints are in the center of the structure or the pathways cross over and under each other), this method will not be guaranteed to help the goal to be reached.

Wall-following can be done in 3D or higher-dimensional mazes if its higher-dimensional passages can be projected onto the 2D plane in a deterministic manner. However, unlike in 2D, this requires that the current orientation be known, to determine which direction is the first on the left or right.

Fig.4 below shows a simple maze which it was use for the basis of illustration how the robot will navigate around it until it exits.

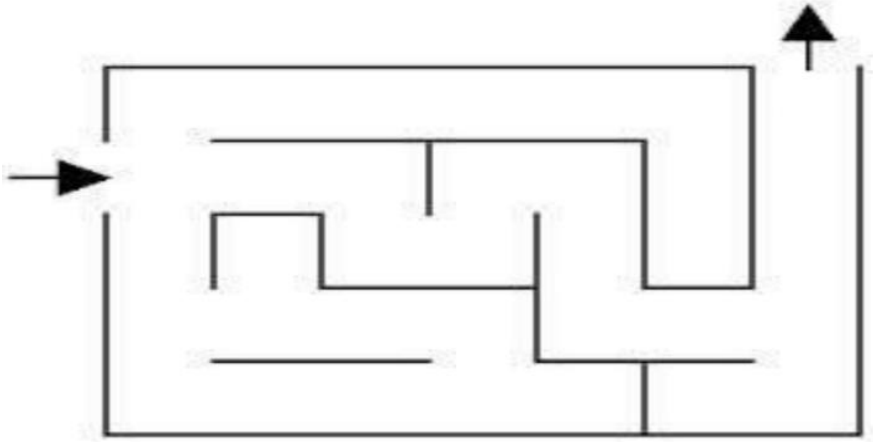

FIGURE 4. Simple Maze for wall follower algorithm

The final implementation was done with the complete system incorporating sensors, the central processing unit and the power supply then couple with the radio controlled toy car was finally done as shown in Fig.5 below.

FIGURE 5. Final implementation

Programming environment

Arduino is a single-board microcontroller, intended to make the application of interactive objects or environments more accessible. The hardware consists of an open-source hardware board designed around an 8-bit Atmel AVR microcontroller, or a 32-bit Atmel ARM. Current models feature a USB interface, 6 analog input pins, as well as 14 digital I/O pins which allow the user to attach various extension boards.

It comes with a simple integrated development environment (IDE) that runs on regular personal computers and allows writing programs for Arduino using C or C++ to the atmega 328 then the chip was transferred to the robot's board. The Fig.6 and Fig.7 below show the Arduino Uno board and the pin mapping for the chip.

FIGURE 6. Arduino Uno Board

FIGURE 7. Atmega pin mapping

SIMULATION RESULT

Simulation of the obstacle sensors

Six obstacle sensors were used to detect the presence of an obstacle in the path of the robot. All of the sensors were similar (they had approximately equal output voltage for a given distance from the obstacle) hence they were having the same response. Fig.8 is the circuit diagram of the obstacle detector designed for the robot.

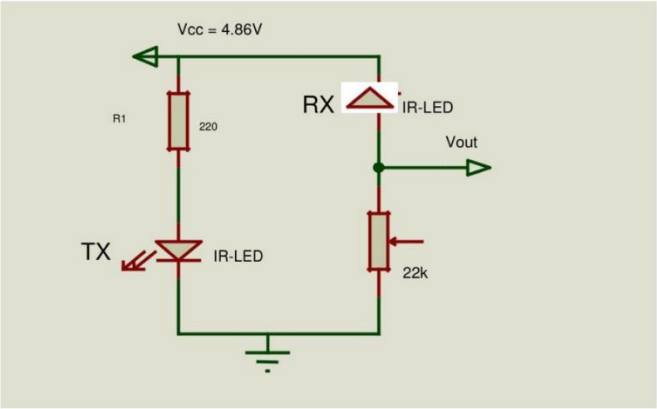

FIGURE 8. Obstacle detector circuit diagram

For Vcc = 4.86V, R1 = 220Ω and R2 = 22KΩ, the obstacle was moved in a straight line along the direction of the obstacle sensor. The corresponding values of the distance of the obstacle from the obstacle sensor (d), and the obstacle sensor's output voltage (Vout) were measured and recorded in table 1.

TABLE 1. Result of the obstacle sensors

Number	Distance, d (cm)	Output Voltage (Volts)
0	No obstacle	1.73
1	35	2.30
2	30	2.41
3	25	2.57
4	20	2.77
5	15	3.03
6	10	3.44
7	5	4.12
8	4	4.35
9	3	4.53
10	2	4.69
11	1	4.70

The plot of the output voltage of the obstacle sensor in volts against the distance of the light source from the sensor in centimeters is as shown in Fig.9.

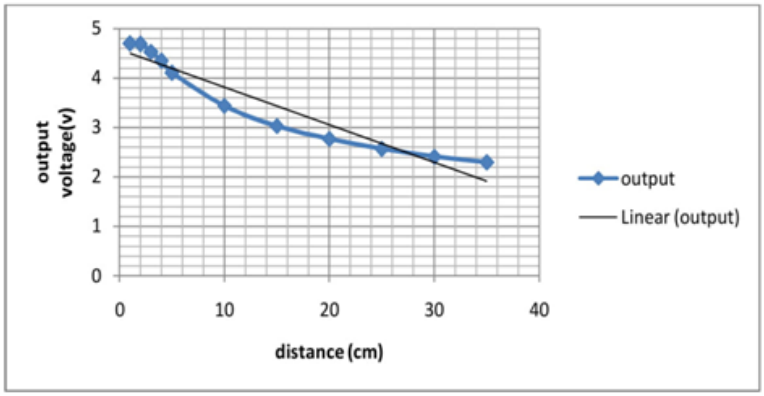

FIGURE 8. Variation of voltage with distance for obstacle sensors

From the plot of the output voltage of the obstacle sensor in volts against the distance of the light source from the sensor in centimeters, it is seen that there is a 1/d^2 variation of distance and the output voltage, with d (cm) being the source distance from the sensor. Therefore as the distance of the obstacle (in the path of the robot) from the sensor decreases the output voltage also increases.

Simulation of the signal processing unit

Output signals from the obstacle detection unit are the inputs to the control signals processing unit. These include the six inputs from the obstacle detectors, which are digital in nature. This implies that the control signals processing unit has six inputs of which are digital in nature.

The test done on the signal processing unit where each one of all of the input signals from all the sensors gave particular instructions as the output of the signal processing unit. Indicated below in table 2 are the various possible states of the robot and the corresponding control action is also suggested.

TABLE 2. States of the robot and the corresponding instructions

Number	Sensor	Instruction
1	Left _forward sensor	Move forward
2	Left _reverse sensor	Move forward with a left turn if left _forward sensor is clear.
3	Forward _left sensor	Move forward with a right turn if the left _forward is blocked
4	Forward _right sensor	Move forward with a right turn if it's not clear, else reverse with left turn until it's clear if all other options are not clear
5	Reverse sensor	Move reverse with left turn until forward right is clear.
6	Right _forward sensor	Move forward with right turn if it's clear and front and left not clear

DISCUSSION

The accuracy value is the most important parameter when conducting a study to detect diarrheal disease because True Positive and True Negative are parameters that will be used as a diagnosis for further treatment. If the accuracy value is too low, the model does not have the ability to distinguish between right and wrong objects, so there is no advantage and will cause harm to sufferers. Model 3 has an accuracy value of 92%, so model 3 is the model that has the highest accuracy value among the other models.

The recall value is the second important parameter because it is the value of the comparison between True Positive and all true actual data. In conducting a study on the detection of diarrhea, the appearance of False Negatives was not expected. False negatives or Escherichia coli bacteria that are negatively detected will be detrimental to the patient because it causes the bacteria to be considered as not Escherichia coli bacteria or considered as another object so that the patient will be considered fine by the doctor. The relationship between recall values and False Negatives in equation 2.12 is inversely proportional, so that the fewer the number of False Negatives, the higher the recall value. Model 3 has a recall value of 95%, so model 3 is the model that has the highest recall value among the other models.

The precision value is an important parameter number three because it is the value of the comparison between the True Positive and all the detection results that the model considers true. In accordance with equation 2.11, if there are fewer False Positives, the precision value will be greater. Even if it is a False Positive or other object that is considered to have a large number of Escherichia coli bacteria, it will actually not be detrimental for sufferers of diarrhea because the patient will immediately be given further treatment by a doctor. Model 3 has a precision value of 96%, so model 3 is the model that has the highest precision value among the other models. and recall, which will be used as an option when the difference between the precision and recall values is too great.

CONCLUSION

In this paper, a maze wanderer robot was designed and implemented using wall follower algorithm technique. Controlling the movement of a robot is necessary for almost all type of robots, thus the device serves as a basic necessity accomplished while designing any high level robots. It was also established that wall follower algorithm has precise control, fast processing, reduced error rate and the most important being cost-effective as compared to depth-first and flood fill algorithms.

REFERENCES

1. K. Maritim, " Maze wanderer robot", Graduation Project, University of Nairobi, Kenya, 2014.
2. A. Kasiman," Optimization algorithm of autonomous maze solving robot", M.Sc. Thesis, Universiti Tun Hussein Onn, Malaysia, 2015.
3. M. Rahman, " Autonomous maze solving robot", Graduation Project, University of Liberal Arts Bangladesh, Bangladesh, 2017.
4. R. Kumar, " Maze solving robot with automated obstacle avoidance", Procedia Computer Science, Vol.105, pp.57-61, 2017.
5. A. Quasmi," Maze-solving robot", VJER-Vishwakarma Journal of Engineering Research, Vol.2, Issue 3, pp. 117-123, 2018.
6. S. Herbie, " Development of a maze solving mobile robot capable of tracking the distance it traversed", Advanced Science Letters, Vol.24, No.11, pp. 8640-864, 2018.

ISSN 2745-3502
Volume 4 No. 1 – Agustus 2023
Indonesian Applied Physics Letters

Application of ANFIS-based Non-Linear Regression Modelling to Predict Concentration Level in Concentration Grid Test as Early Detection of ADHD in Children

Sayyidul Istighfar Ittaqillah [1a)], Delfina Amarissa Sumanang [1b)], Quinolina Thifal[1c)], Akila Firdausi Harahap[1d)], Akif Rahmatillah[1,2e)], Alfian Pramudita Putra[1,2f)], Riries Rulaningtyas[1,2g)], Osmalina Nur Rahma[1,2h)]

[1]Biomedical Engineering Study Program, Department of Physics, Faculty of Science and Technology, Universitas Airlangga, Indonesia
[2]*Medical Signal and Robotic Research Group, Universitas Airlangga, Indonesia*

[a)]sayyidul.istighfar.ittaqillah-2020@fst.unair.ac.id
[b)]delfina.amarissa.sumanang-2020@fst.unair.ac.id
[c)]quinolina.thifal-2020@fst.unair.ac.id
[d)]akila.firdausi.harahap-2020@fst.unair.ac.id
[e)]akif-r@fst.unair.ac.id
[f)]alfian.pramudita@fst.unair.ac.id
[g)]riries-r@fst.unair.ac.id
[h)]Corresponding Author: osmalina.n.rahma@fst.unair.ac.id

Abstract. Concentration is the main asset for students and serves as an indicator of successful learning implementation. One of the abnormal disturbances that can occur in a child's concentration development is attention deficit hyperactivity disorder (ADHD). The prevalence of ADHD in Indonesia in 2014 reached 12.81 million people due to delayed management in addressing ADHD. Therefore, early detection of ADHD is necessary for prevention. ADHD detection can be done by testing the level of concentration using a concentration grid. However, a method is needed that can be applied to uncooperative young children who are not familiar with numbers. Therefore, research was conducted with an innovative approach using a combination of EEG-ECG to classify concentration levels. The data used in this study were primary data from 4 participants with 5 repetitions. The data were processed in the preprocessing stage, which involved noise filtering and Butterworth filtering. The features used in this study were BPM (beats per minute), alpha, theta, and beta EEG signals, which would later become inputs for the Adaptive Neuro-Fuzzy Inference System (ANFIS). The output shows that the combination of EEG-ECG has the potential to predict concentration test results. Using BPM, alpha, theta, and beta signals can serve as parameters for predicting the concentration grid test values using ANFIS effectively. In the ANFIS model with 4 features, an accuracy of 99.997% was obtained for the training data and 80.2142% for the testing data. This result could be developed for early detection of ADHD based on concentration levels so the learning implementation could be more effective.

Keywords: Concentration Level, ADHD, ECG, EEG, ANFIS

INTRODUCTION

Concentration is the focus of attention in the process of changing behavior which is expressed in the form of mastery, use, and evaluation of attitudes and values, basic knowledge and skills contained in various fields of study. If a student's concentration is low, it will also lead to low-quality activities and can lead to not being serious in learning. That lack of seriousness affects the power of understanding the material. Concentration is the main capital for students in receiving

material and is an indicator of successful implementation of learning [3]. Learning in public schools where children live is the first step in building the future of this country. However, not all children are in good health and experience abnormal behavior disorders. One of the abnormal disorders that occur in child development is Attention Deficit Hyperactivity Disorder or ADHD. ADHD is a developmental disorder that increases motor activity in children, causing excessive and unusual activity [4].

Based on the American Psychiatric Association (2013), ADHD is described as a neurodevelopmental disorder with persistent behavior patterns in the form of lack of concentration and/or excessive hyperactivity/impulsivity [1]. In Indonesia, research on the prevalence rate of ADHD was conducted which stated that the prevalence of ADHD in Indonesia was 5% or around 12.81 million people of Indonesia's population [5]. Lack of parental knowledge about ADHD can result in slow treatment to overcome ADHD. In general, individuals who suffer from ADHD as children will inhibit some of these traits as adults such as difficulty focusing or concentrating on one activity. Therefore, prevention needs to be done by doing early detection of ADHD.

The simplest detection of ADHD is to test the concentration level of the children. Testing the level of concentration can be done in various ways. The most common way to do this is with a concentration grid. This method is done by ordering the numbers from 0 to 99 or from 1 to 100. However, this method cannot be done on children who are uncooperative in testing and also children who still cannot recognize numbers. ADHD detection needs to be done as early as possible so that concentration grid testing cannot be done. It is hoped that this research can detect ADHD as early as possible in order to reduce sufferers and improve the quality of life and education according to SDGs number 3 and 4. Therefore, a method that can be done on young children who are uncooperative and don't know numbers is needed. So an innovation was made for concentration testing using EEG and ECG.

EEG and ECG are used by combining the two signals as information to replace the concentration grid test. Based on research, a combination of EEG and ECG was carried out to determine the level or level of concentration in children using the Adaptive Neuro-Fuzzy Inference System (ANFIS). The results of the ANFIS training that has been carried out provide an accuracy value of 80.69% for training data and 65.88% for test data. This study uses EEG information in the form of changes in Max. Alpha and BPM change information from the ECG between normal conditions and concentration conditions [6]. Another research showed that theta and beta signals from the EEG had an effect on concentration. This is the basis for the development of ANFIS by using inputs in the form of BPM values, alpha, theta, and beta signals to determine the replacement value for the concentration grid level [7]. This research is expected to provide results in accordance with the concentration grid test by utilizing the EEG-ECG combination. In addition, with this innovation, it is hoped that the detection of ADHD can be done as early as possible in order to reduce sufferers and improve the quality of life and education according to SDGs number 3 and 4.

RESEARCH METHODOLOGY

In general, the research scheme is shown in Figure 1 by conducting the EEG and ECG signal from subjects then processing the features into the classifier. The result was also compared with the concentration grid to verify the concentration level of the subject.

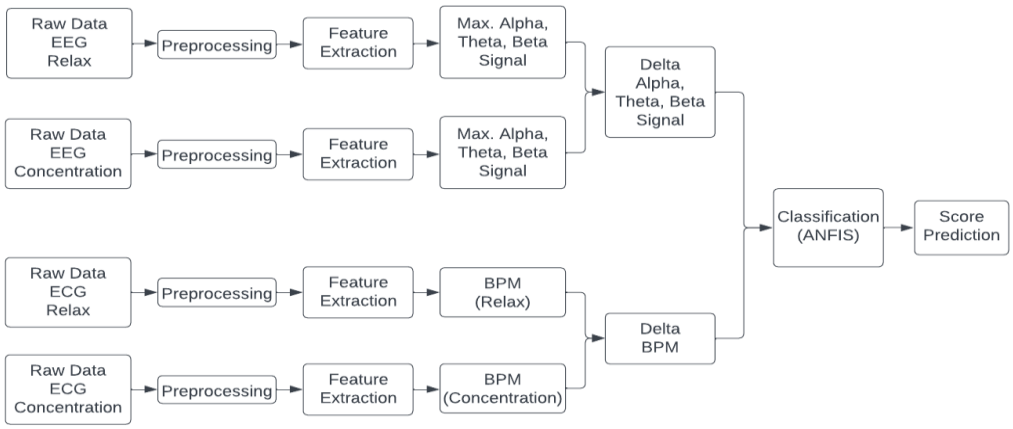

FIGURE 1. Research scheme flowchart

Data Collection

The data were collected from 4 subjects (male, 20 years age). In this research, each participant underwent five data collection sessions. During each session, simultaneous ECG and EEG data recording was performed using the BITalino device. The data was recorded for a duration of one minute, utilizing the autosave feature of the BITalino. For data acquisition, a specialized BITalino cable with three branches was used. The cable was color-coded, with red indicating the positive pole, black representing the negative pole, and white serving as the ground. The EEG electrodes were placed on the frontal part, specifically FP1 and FP2, with the ground electrode positioned behind the ear. These locations (FP1 and FP2) are known for their rich information content and their potential to identify concentration states [8]. The electrode placement is shown in Figure 2.

The data collection process consisted of two conditions: relaxation and concentration. During the relaxation condition, the participants will be in a relaxed state to assess the brain's activity. They will listen to specifically selected songs that promote relaxation while keeping their eyes closed. Listening to music has been shown to induce a relaxed state without causing drowsiness [9].

FIGURE 2. Electrode placement for (a) ECG and (b) EEG

The subjects were asked to do a concentration grid test (10 rows x 10 columns) during the concentration condition. The procedure consists of ordering numbers from 1 to 100 in ascending order [6]. Each participant was given one minute to do the test; their score will be the last number they reached. The assumption is that the more numbers an individual is able to order, the higher their concentration level is.

Signal Pre-Processing

The ECG signal was captured using the Bitalino software with the aVR lead configuration. The obtained data was saved as a .txt file for easy access and analysis. To enhance the data quality, a preprocessing stage was applied. The raw data went through a high-pass filter implemented with a Butterworth filter. This filtering process effectively eliminates the baseline drift present in the raw data. The Butterworth filter used is a commonly employed Infinite Impulse Response (IIR) filter in signal processing. In this case, a second-order filter with a cutoff frequency of 0.5 Hz was utilized. By implementing this filter, the detection and analysis of ECG waves associated with cardiac activity are significantly improved.

While for the raw EEG signal, the pre-processing involves eliminating noise and artifacts and enhancing the relevant signal components. This process ensures that subsequent analysis focuses on the brain's electrical activity and minimizes interference from external factors or physiological artifacts. The steps in the EEG preprocessing stage are; data selection, frequency sampling, filter design, filter coefficient, and filter application.

1. Data Selection

   The input data is assumed to be called a *data* matrix in the code, where each column represents a different signal. Biosignal The EEG is recorded in the 7th column of the data matrix. This selected EEG data is then assigned to a variable *eeg*. Additionally, to limit the analysis to a certain subset of data, the code truncates the EEG data to the first 45,000 samples of the data. This is because there are variations in the amount of recorded data obtained so the EEG data is limited to the first 45,000 samples to ensure consistency and fairness in data processing.
2. Sampling Frequency

   The code sets the sampling frequency (*fs*) to 1000 Hz, adjusting the BITalino setting during data capture. This value represents the number of samples recorded per second in the EEG signal.
3. Filter Design

   At this step, the bandpass filter Butterworth is designed for different frequency bands: alpha, theta, and beta. The butter function is used to design this filter, and the desired filter order is set to 3. Each frequency band is associated with a specific physiological phenomenon or brain activity.
4. Filter Coefficient

   The code calculates the filter coefficient based on filter design specifications and sampling frequency using the butter function to perform the actual filtering operation. This coefficient captures the filter characteristic for which it

is designed and required for the next filtering step.

5. Filters Application

The designed filter is applied to the EEG signal using the '*filterfilt*' function. This function performs zero-phase forward and reverse filtering to remove any phase distortion that can occur during filtering. The filtered signal is then stored separately. Each variable stores the EEG signal, which is filtered according to a certain frequency band.

Feature Extraction

In the feature extraction phase, the R peaks of the aVR lead ECG signal are identified using the "*findpeaks*" algorithm. To ensure the accuracy of the detected peaks, a minimum peak height criterion, set at 0.3, is employed. Only peaks that reach this height threshold are considered valid R peaks. Any peaks falling below this threshold are disregarded.

To maintain appropriate spacing between the detected peaks, the "*MinPeakDistance*" parameter is utilized. It determines the minimum allowable distance between peaks during the search process. Specifically, the minimum distance is set as 0.6 times the sampling rate (fs) of the ECG signal. Consequently, peaks occurring closer to each other than 0.6 seconds are discarded to avoid double counting or misinterpretation.

Subsequently, measurements are conducted to calculate the time difference between consecutive R peaks on the ECG signal. This time difference is then converted from seconds to beats per minute (BPM) using appropriate formulas.

EEG, a non-invasive neuroimaging technique, enables the measurement of bioelectrical activity in the brain. EEG values are widely employed in neuroscience, psychology, and medicine and offer valuable insights into brain function and activity [10]. EEG signals provide valuable insights into various mental states, including concentration and relaxation. Feature extraction in EEG focuses on identifying and extracting relevant characteristics, which in this case is power spectral density and signal amplitude. It can reveal dominant frequency bands and overall brain activity patterns that are very important for identifying the characteristics of mental states of concentration and relaxation.

The steps in the EEG feature extraction stage are; amplitude extraction, *power spectral density* (PSD) calculation, extraction of the maximum value per EEG frequency band, and normalization.

1. Amplitude Extraction

The code uses Fast Fourier Transform (FFT) to calculate the amplitude of each filtered signal. FFT is applied to each filtered signal, `alpha_filtered`, `theta_filtered`, and `beta_filtered`, using the function `fft`. The result of the FFT operation is stored in a separate variable (`for`, `zt`, and `zb`).

2. Power Spectral Density (PSD) Calculation

The power spectral density is calculated based on the amplitude information obtained from the FFT. For each filtered signal (`alpha_filtered`, `theta_filtered`, and `beta_filtered`), the code calculates the power spectral density by squaring the absolute value of the FFT result. This is done using `abs` operation and `.^2`. The resulting power spectral density signal is stored in a separate variable (`PSa`, `PSt`, and `PSb`).

3. Extraction of Maximum Value per EEG Frequency Band

The code extracts the maximum value for each frequency band from the power spectral density signal. The maximum value represents the dominant power in a certain frequency range. To achieve this, the code uses the `max` function to find the maximum value of each power spectral density signal (`max(PSa)`, `max(PSt)`, and `max(PSb)`).

4. Normalization

The maximum values extracted are normalized by dividing by 10^10 to ensure consistent and concise feature values. This normalization step helps scale feature values appropriately. Additionally, normalized feature values are rounded to two decimal places for clarity and precision. The resulting normalized and summarized feature values are stored in separate variables (`maxAlpha`, `maxTheta`, and `maxBeta`).

Classification

The Adaptive Neuro-Fuzzy Inference System (ANFIS) is a machine learning approach that combines adaptive network systems with fuzzy system approximation. It utilizes a Sugeno fuzzy model trained using an adaptive network. This hybrid learning procedure enables modeling even in scenarios where expert knowledge is limited.

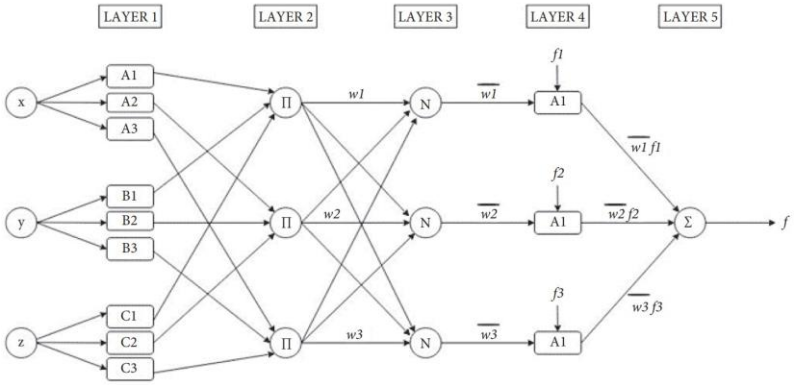

FIGURE 3. ANFIS architecture

ANFIS consists of 5 layers, each serving a specific function. The first layer is the fuzzification layer responsible for generating fuzzy sets using membership functions. The second layer is the implication layer, where the weights of the fuzzy rules are determined. The third layer is the normalizing layer, which displays the standard activation degree and normalizes the weights from the second layer. The fourth layer is the defuzzification layer, which is adaptive and computes the weighted multiplication of the previous layer's outputs. The final layer is the output or combining layer, where the results from the previous layers are summed [11].

Data evaluation is performed to assess the accuracy of the developed ANFIS system. The evaluation of ANFIS using regression model methods can utilize RMSE (Root Mean Square Error), MSE (Mean Square Error), and MAPE (Mean Absolute Percentage Error) [12]. RMSE indicates the magnitude of prediction errors. A smaller RMSE value, closer to 0, indicates more accurate predictions [13]. The MSE and MAPE methods are also employed to test the errors of each prediction system. The system with the smallest MSE and MAPE values is considered the best for making predictions [14]. MAPE values have specific ranges to assess the predictive capabilities of the model. Lower MAPE values indicate better prediction performance [15].

RESULT AND DISCUSSION

Based on the applied ECG processing that consists of two stages; preprocessing and feature extraction, the results are obtained in the form of BPM (beats per minute) of the heart rate. Heart rate (or pulse) is the frequency of heartbeats as measured by the number of heart contractions per minute (beats per minute, or bpm). The results of the bpm from several participants ranged from 71 - 76 bpm in a state of relaxation and 71 - 86 BPM in a state of concentration. This is in accordance with the American Heart Association, which states that the normal adult human heart rate at rest is 60-100 bpm.

During relaxation, the heart rate tends to decrease when the body is at rest, and the mind is calm. This is because the body's overall metabolic activity is lower, and the parasympathetic nervous system, which is responsible for promoting relaxation and recovery, becomes more active. Based on Figure 4, heart rate is often at the lower end of the normal range (about 60 to 80 bpm) while in a relaxation state. On the other hand, during mental concentration or focus, the heart rate may increase slightly. This is caused by activating the sympathetic nervous system, which is responsible for the response fight-or-flight body. When in a state of concentration that requires attention and focus, the body releases certain stress hormones that can increase heart rate and blood pressure. The increase in heart rate during concentration is usually not very high and can vary depending on the individual and the intensity of mental activity. However, the difference in heart rate between relaxation and concentration can vary between individuals. Factors such as overall fitness level, stress level, and underlying health conditions can affect variations in heart rate during different circumstances.

The experimental results showed differences in heart rate in different relaxation and concentration conditions. In some data, the heart rate in a relaxed state is higher than in a state of concentration. This is due to the accurate data collection when the relaxation state is due to the person only sitting in a room that is quite open. In addition, the program code for removing noise by filter and determining height and distance peak also affect the corresponding heart rate results.

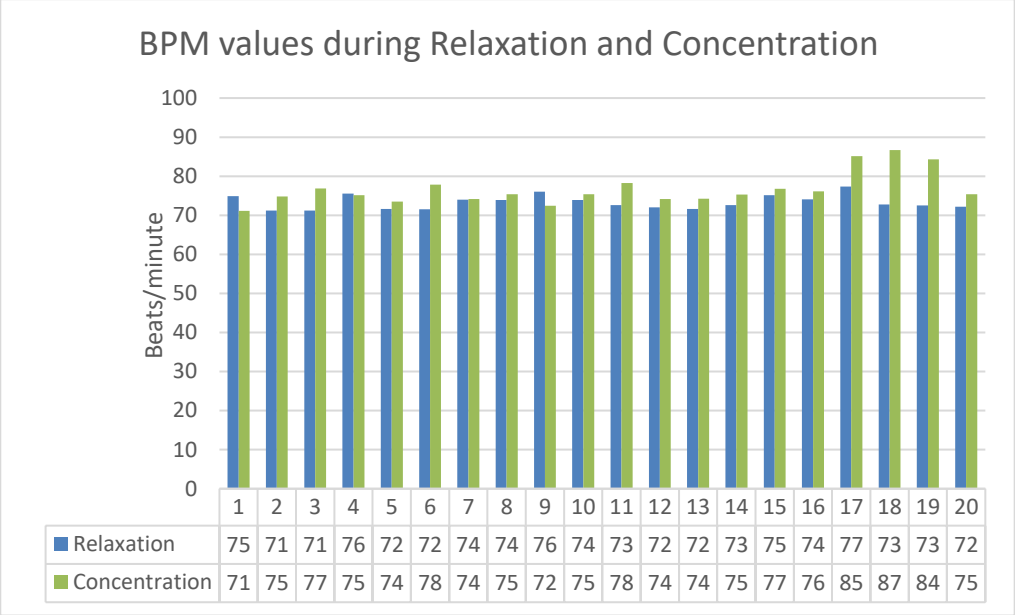

	1	2	3	4	5	6	7	8	9	10	11	12	13	14	15	16	17	18	19	20
Relaxation	75	71	71	76	72	72	74	74	76	74	73	72	72	73	75	74	77	73	73	72
Concentration	71	75	77	75	74	78	74	75	72	75	78	74	74	75	77	76	85	87	84	75

FIGURE 4. BPM values during relaxation and concentration

The result of the EEG processing stage, preprocessing, and feature extraction was obtained in the form of PSD (power spectral density) of the alpha, theta, and beta waves (Figure 5). During relaxation, it has been observed that alpha waves tend to increase in amplitude. Alpha waves are usually present in the 8-13 Hz frequency range and are associated with a relaxed and calm state of mind. An increase in alpha strength indicates a decrease in mental activity and can be an indication of a relaxed state [16]. During relaxation, the increase in the amplitude of alpha waves can be related to the physiological aspects of the brain's electrical activity. Alpha waves primarily originate in the thalamus, a brain structure involved in organizing sensory information. Increased alpha strength reflects decreased processing of sensory input and reduced cognitive engagement. This physiological state is associated with a relaxed and calm mental state [17].

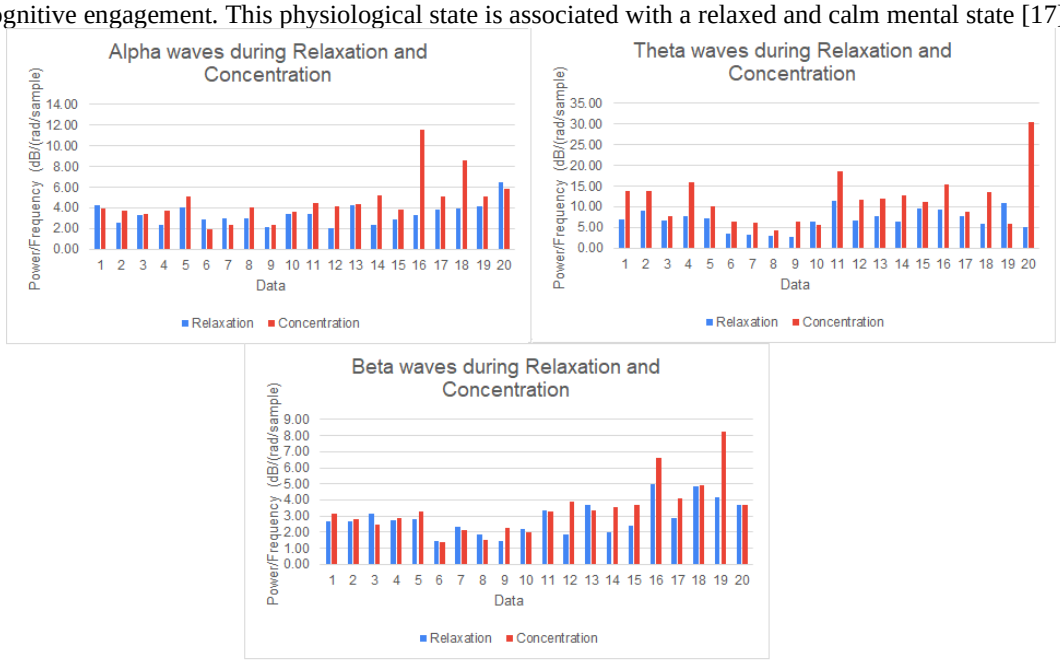

FIGURE 5. Power spectral density from several brain waves during relaxation and concentration

On the other hand, during concentration or cognitive engagement, it is often observed that alpha waves decrease in amplitude, whereas beta waves increase. Beta waves are generally associated with increased mental activity, focus and alertness. They have a frequency range of 13-30 Hz, and higher beta strength is associated with increased concentration and cognitive processing [16]. During concentration, the concomitant decrease in the amplitude of alpha waves and

increase in beta waves can be explained by the increased cognitive processing demands of the brain. The neocortex, the brain's outer layer responsible for higher cognitive functions, generates beta waves. A decrease in alpha strength signals a shift from a relaxed state to a more focused and alert mental state. Increased beta power corresponds to increased cortical activation and increased cognitive processing, supporting concentration and mental engagement [18].

The theta waves, which are in the 4-8 Hz frequency range, are often associated with deep relaxation, meditation, and sleepiness. These waves tend to increase during states of deep relaxation or meditation [16]. Theta waves, on the other hand, play a role in states of deep relaxation, meditation, and sleepiness. An increase in theta power during deep relaxation or meditation is linked to decreased awareness and increased introspection. These waves are thought to originate from the limbic system and hippocampus, which are involved in emotional processing and memory consolidation. The increase in theta power during relaxation reflects the physiological changes associated with a more introspective and meditative state [19].

From this reference, we perform the calculation of alpha in a relaxed state minus alpha in a concentrated state (assuming higher relaxed alpha), theta in a relaxed state minus theta in a concentrated state (assuming theta in a higher relaxed state), beta in a relaxed state. concentrated minus beta in a relaxed state (assuming beta is in a higher concentrated state) for each data collection. The difference between relaxed alpha and intense alpha ranges from 0.35 to -8.28. The difference between relaxed theta and intense theta ranges from -25.55 to 4.88. The difference between concentrated beta and relaxed beta ranges from -0.69 to 4.07.

If we compare to the literature, there are some anomalies in the data that can be related to several factors, such as individual differences, cognitive strategy, measurement error, or other factors. Brain wave activity can vary significantly between individuals. Everyone has different neurophysiological characteristics, and their brain waves may respond differently to relaxation and concentration. These individual differences can manifest as anomalies in the data, where some individuals may show unexpected patterns or deviate from the general trend observed in the data set. Anomalies may also arise from various cognitive strategies used by individuals during concentration. People may use various approaches or mental techniques to increase their focus and concentration, which causes variations in brain wave activity. These strategies can involve different levels of mental effort, attention allocation, or cognitive control, which can influence the observed differences in alpha, theta, and beta strength. Measurement errors and other factors, such as environmental factors and emotional or physical condition, during data collection or analysis could also contribute to the anomaly of data.

After extracting all the features, we calculated the difference values from relaxation and concentration as input for ANFIS. So, the input became delta BPM, delta maximum Alpha, delta maximum Delta, and delta maximum Theta, as shown in Table 1 and Table 2. The predicted and actual results also show a slight difference in the resulting values. This difference was then also analyzed based on 4 data evaluation parameters, namely the value of RMSE, MSE, MAPE, and accuracy (Table 3).

TABLE 1. ANFIS Train Data Result

Training Data	Input				Actual	ANFIS Prediction
	BPM	Max. Alpha	Max. Theta	Max. Beta		
1	-3.81	0.35	-6.73	0.48	19.00	19.00
2	3.58	-1.21	-4.79	0.13	18.00	18.00
3	5.63	-0.17	-0.88	-0.69	18.00	18.00
4	-0.42	-1.32	-8.04	0.12	17.00	17.00
5	1.88	-1.08	-2.96	0.52	22.00	21.99
6	6.30	0.92	-2.83	-0.09	21.00	20.99
7	0.11	0.61	-2.89	-0.24	19.00	18.99
8	1.52	-1.11	-1.40	-0.35	23.00	22.99
9	-3.62	-0.25	-3.59	0.84	21.00	20.99
10	1.44	-0.17	0.59	-0.21	17.00	17.00

TABLE 2. ANFIS Test Data Result

Testing Data	Input				Actual	ANFIS Prediction
	BPM	Max. Alpha	Max. Theta	Max. Beta		
1	5.65	-1.04	-7.21	-0.13	19.00	14.76
2	2.19	-2.07	-5.05	2.04	12.00	19.91
3	2.63	-0.14	-4.05	-0.34	18.00	21.65
4	2.76	-2.84	-6.24	1.57	17.00	18.03
5	1.59	-1.01	-1.51	1.32	21.00	23.52
6	2.01	-8.28	-5.91	1.67	17.00	20.00
7	7.76	-1.36	-0.87	1.18	22.00	19.99
8	13.95	-4.60	-7.82	0.04	17.00	20.00
9	11.77	-0.98	4.88	4.07	22.00	20.00
10	3.24	0.62	-25.55	-0.01	17.00	20.00

TABLE 3. ANFIS Test Data Result

Data	RMSE	MSE	MAPE (%)	Accuracy (%)
Training	0.0001	0.0000	0.0008	99.9970
Testing	3.6900	13.6500	17.6500	80.2142

Based on the RMSE and MSE values from the ANFIS 4 feature training, a small value is obtained or close to 0. This value indicates that the predicted model that has been trained has a small error. The MAPE value of the 4 feature training data is less than 10%, which means that the predictive model's ability to train is very good. Calculating accuracy in ANFIS training with these 4 features produces an accuracy of 99.99% for training and 80.21% for testing. Based on the table it can also be seen that for each number of features for ANFIS training contributes to obtaining high accuracy. However, the test data obtained higher error values and lower accuracy than the training data. However, all of these values are still in the range of values, proving that the predictions made are good.

CONCLUSION

Based on research that has been done, the combination of EEG and ECG has the potential to be a substitute for the concentration grid test to predict concentration test scores. The use of BPM values, alpha, theta, and theta signals can be good parameters for predicting concentration grid test values using ANFIS. A higher accuracy value supports this compared to research with similar methods and has low RMSE, MSE, and MAPE values. Whereas ANFIS 4 features obtained an accuracy of 99.997% for training data and 80.2142% for test data is obtained. This result could be developed for early detection of ADHD based on concentration levels so the learning implementation could be more effective.

REFERENCE

1. American Psychiatric Association, DSM-5 Classification, 5th ed. American Psychiatric Association, 2016.
2. “Siapakah yang Berpotensi Sebagai Penyandang ADHD,” Pusat Kemandirian Anak, Jun. 21, 2018. https://pusatkemandirianank.com/siapakah-yang-berpotensi-sebagai-penyandang-adhd/ (accessed Jun. 19, 2023).
3. R. Aviana and F. F. Hidayah, “PENGARUH TINGKAT KONSENTRASI BELAJAR SISWA TERHADAP DAYA PEMAHAMAN MATERI PADA PEMBELAJARAN KIMIA DI SMA NEGERI 2 BATANG,” J. Pendidik. SAINS Univ. MUHAMMADIYAH SEMARANG, vol. 3, no. 1, Art. no. 1, 2015, doi: 10.26714/jps.3.1.2015.30-33.
4. F. Suryani and A. Iswardani, “SISTEM PAKAR DIAGNOSIS JENIS PERILAKU ATTENTION DEFICIT HYPERACTIVITY DISORDER PADA ANAK DENGAN METODE CERTAIN FACTOR,” Proceeding SENDIU, Dec. 2018, Accessed: Jun. 19, 2023. [Online]. Available: https://www.unisbank.ac.id/ojs/index.php/sendi_u/article/view/5980
5. F. R. Roshinah, L. Nursaliha, and S. Amri, “PENGARUH TERAPI MUROTTAL TERHADAP TINGKAT HIPERAKTIF – IMPULSIF PADA ANAK ATTENTION DEFICIT HYPERACTIVE DISORDER (ADHD),” Pelita - J. Penelit. Mhs. UNY, vol. 9, no. 02, Art. no. 02, 2014, Accessed: Jun. 19, 2023. [Online]. Available: https://journal.uny.ac.id/index.php/pelita/article/view/4017
6. A. B. H. Tanjung, I. P. Wibawa, and H. Mukhtar, “Analisis Tingkat Konsentrasi Berpikir Manusia Berdasarkan Eeg Dan Ekg Menggunakan Adaptive Neuro Fuzzy Inference System,” EProceedings Eng., vol. 7, no. 1, 2020.
7. “Comparison between Concentration and Immersion Based on EEG Analysis”, Accessed: Jun. 19, 2023. [Online]. Available: https://www.mdpi.com/1424-8220/19/7/1669

8. T. J. Choi, J. O. Kim, S. M. Jin, and G. Yoon, "Determination of the Concentrated State Using Multiple EEG Channels," Int. J. Biomed. Biol. Eng., vol. 8, no. 8, pp. 1373–1376, 2014.
9. D. Djohan, F. Tyasrinestu, and L. A. E. Sualang, "Pengaruh Mendengarkan Musik Terhadap Kondisi Rilaksasi," ResitalJurnal Seni Pertunjuk., vol. 23, no. 3, Art. no. 3, Dec. 2022, doi: 10.24821/resital.v23i3.8337.
10. S. Sanei and J. A. Chambers, EEG signal processing. John Wiley & Sons, 2013.
11. S. Chopra, G. Dhiman, A. Sharma, M. Shabaz, P. Shukla, and M. Arora, "Taxonomy of Adaptive Neuro-Fuzzy Inference System in Modern Engineering Sciences," Comput. Intell. Neurosci., vol. 2021, p. 6455592, Sep. 2021, doi: 10.1155/2021/6455592.
12. O. M. Olatunji, I. T. Horsfall, E. Ukoha-Onuoha, and K. Osa-aria, "Application of hybrid ANFIS-based non-linear regression modeling to predict the% oil yield from grape peels: Effect of process parameters and FIS generation techniques," Clean. Eng. Technol., vol. 6, p. 100371, 2022.
13. M. Mahyudin, I. Suprayogi, and T. Trimaijon, "Model Prediksi Liku Kalibrasi Menggunakan Pendekatan Jaringan Saraf Tiruan (ZST)(Studi Kasus: Sub DAS Siak Hulu)," J. Online Mhs. JOM Bid. Tek. Dan Sains, vol. 1, no. 1, pp. 1–18, 2014.
14. I. Sungkawa and R. T. Megasari, "Penerapan ukuran ketepatan nilai ramalan data deret waktu dalam seleksi model peramalan volume penjualan pt satriamandiri citramulia," ComTech Comput. Math. Eng. Appl., vol. 2, no. 2, pp. 636–645, 2011.
15. M. A. Maricar, "Analisa perbandingan nilai akurasi moving average dan exponential smoothing untuk sistem peramalan pendapatan pada perusahaan xyz," J. Sist. Dan Inform. JSI, vol. 13, no. 2, pp. 36–45, 2019.
16. S. Lim, M. Yeo, and G. Yoon, "Comparison between Concentration and Immersion Based on EEG Analysis," Sensors, vol. 19, no. 7, 2019, doi: 10.3390/s19071669.
17. W. Klimesch, P. Sauseng, and S. Hanslmayr, "EEG alpha oscillations: the inhibition-timing hypothesis.," Brain Res. Rev., vol. 53, no. 1, pp. 63–88, Jan. 2007, doi: 10.1016/j.brainresrev.2006.06.003.
18. P. J. Uhlhaas and W. Singer, "Neural Synchrony in Brain Disorders: Relevance for Cognitive Dysfunctions and Pathophysiology," Neuron, vol. 52, no. 1, pp. 155–168, 2006, doi: https://doi.org/10.1016/j.neuron.2006.09.020.
19. L. Thompson and M. Thompson, "Chapter 14 - QEEG and neurofeedback for assessment and effective intervention with attention deficit hyperactivity disorder (ADHD)," in Introduction to Quantitative EEG and Neurofeedback (Second Edition), T. H. Budzynski, H. K. Budzynski, J. R. Evans, and A. Abarbanel, Eds., Second Edition. San Diego: Academic Press, 2009, pp. 337–364. doi: https://doi.org/10.1016/B978-0-12-374534-7.00014-9.
.

ISSN 2745-3502
Volume 4 No. 1 – Agustus 2023
Indonesian Applied Physics Letters

Classification of Pneumonia from Chest X-ray Images Using Keras Module TensorFlow

Franky Chandra Satria Arisgraha[1,a)], Riries Rulaningtyas[1], Miranti Ayudya Kusumawardani[1]

[1] Biomedical Engineering, Faculty of Science and Technology, Universitas Airlangga, Surabaya, Indonesia

[a)] Corresponding author: franky-c-s-a@fst.unair.ac.id

Abstract. Pneumonia is a respiratory disease caused by bacteria and viruses that attack the alveoli, causing inflammation of the alveoli. This study aims to examine the ability of the Convolutional Neural Network (CNN) model to classify pneumonia and normal x-ray images. The method used in this research is to construct a CNN model from scratch by compiling layers one by one with the help of the Keras TensorFlow module, which consists of a Convolution layer, MaxPooling layer, Flatten layer, Dropout layer, and Dense layer. Data used in this research is from Guangzhou Women and Children Medical Center, Guangzhou, China. The total data used is 200 images divided into 160 test data, 20 training data, and 20 validation data. From the results of the research conducted, the model has the fastest processing speed of 9.6ms/epoch with a total of 20 epochs. The model has the highest accuracy value of 77% in the training process and an accuracy value of 80% in the testing process. The highest sensitivity value is 1.54 in training and 1.6 in testing. The highest specificity value is 0.77 in training and 0.8 in testing. It can be said that the model can do good classification. Pendahuluan / Introduction (first level heading).

INTRODUCTION

Pneumonia is an infection that causes inflammation of the alveoli and their filling with fluid or pus in one or both lungs (Franquet, 2018). Consequently, patients experience productive cough, fever, chills, chest pain, and difficulty breathing. Pneumonia can be caused by bacteria, viruses, or fungi, with bacterial infections being most common in adults. Pneumonia is a leading cause of death among children worldwide. The World Health Organization (WHO) estimates that this disease accounts for 15% of deaths in children under 5 years old (WHO, 2020). Annually, pneumonia affects approximately 450 million people, representing seven percent of the global population, and leads to around 4 million deaths. In Indonesia, based on the Basic Health Research (Riskesdas) conducted by the Ministry of Health in 2018, the estimated number of pneumonia cases accounts for 2% of the total population. This indicates a 0.2% increase from 2013 when it was 1.8% (Kemenkes, 2018).

Early detection of pneumonia is crucial for providing appropriate medical care to patients. One common technique for early detection involves the examination of X-ray thorax images by radiologists or physicians. However, this method has inherent weaknesses due to subjectivity, influenced by the reader's expertise, fatigue, and visual acuity. To address the limitations of traditional reading techniques, researchers have experimented with building a pneumonia X-ray image classification model using machine learning. Stephen et al. employed a deep learning model, Convolutional Neural Network, comprising 4 Convolutional layers, 4 MaxPooling layers, 1 Flatten layer, and 7 Dense layers, with additional input variations such as scaling, rotation, width shift, height shift, shear range, zoom range, and horizontal flip (Stephen et al., 2019). The results demonstrated an accuracy rate of 93%. Jain et al. tested several Convolutional Neural Network (CNN) models, including VGG16, VGG19, ResNet50, and Inception-v3, for pneumonia detection (Jain et al., 2020). All four CNN methods used showed effectiveness in feature extraction and automatic classification. The best performance was observed with RestNet50. Xiang Xu conducted experiments to obtain optimal feature extraction using the Graph-Knowledge Embedded CNN method (Yu et al., 2020). Combining features extracted using two different methods with graph-based feature reconstruction, Xiang Xu et al. achieved an accuracy of 98%.

Based on this information, the authors aimed to build a CNN model capable of lightweight X-ray pneumonia image classification with high accuracy and efficiency using the Keras API based on the TensorFlow framework. The Keras API is an interface library designed to simplify the implementation of deep learning algorithms, reducing the required number of steps for code implementation running on TensorFlow (Chollet, F., 2015). TensorFlow itself is an open-source library created by the Google Brain team, utilized for large-scale numerical computations and machine learning projects, including deep learning (neural networks) (TensorFlow, 2018). Utilizing TensorFlow and Keras API aims to maximize research efficiency. The constructed Convolutional Neural Network (CNN) structure in this study comprises 6 convolutional layers, with 1 initial layer serving as input, 5 MaxPooling layers, 1 Flatten layer, 1 Dropout layer, and 2 Dense layers utilizing ReLu activation for convolution layers and softmax for classification (Dense) layer. The dataset used consists of X-ray images of pneumonia and normal cases obtained from female patients aged one to five years from the Guangzhou Women and Children's Medical Center, Guangzhou, China (Mooney, 2019)..

RESEARCH METHODOLOGY

Data

Chest X-Ray (CXR) or chest radiography is one of the most commonly used medical imaging applications for disease detection, including pneumonia. X-ray images can reveal areas of opacity or obstruction with brighter shades on the image. During the data collection phase, the best dataset with a high quantity and diversity of data was sought and compared. After selecting the suitable dataset, it was downloaded from the link provided: https://www.kaggle.com/datasets/paultimothymooney/chest-xray-pneumonia. This dataset comprises X-ray images of pediatric patients aged one to five years from the Guangzhou Women and Children's Medical Center, Guangzhou, China (Mooney, 2019). Next, the data was examined and organized according to the defined scope, which consists of a total of 200 images distributed in an 80:10:10 ratio. Specifically, there are 160 training data, comprising 80 pneumonia and 80 normal images. Additionally, there are 20 test data, with 10 pneumonia and 10 normal images, and 20 validation data, consisting of 10 pneumonia and 10 normal images.

Design and Construction of the Model Structure

This research was conducted using Google Colaboratory, a cloud-based text editor. This application runs within a web browser, eliminating the need for installation on the user's device. The programming language used in this study is Python, with the TensorFlow library and the Keras API module. First, we conduct a preprocessing data. In the data preprocessing stage, data augmentation is performed on the image size and various image transformations. Image augmentation is a technique that applies different transformations to an image, resulting in multiple transformed copies of the same image, thereby expanding the dataset (Bharati, S., 2020).

The method used involves extracting data arrays from an image using the Image Data Generator function provided by the Keras library, allowing the data to be read by the CNN model that has been prepared. In this step, the image data is standardized to a uniform size by scaling the data to 1/255 and applying horizontal flip to introduce data variation. This research utilizes the Keras API, making use of several available layer classes, namely Sequential, Convolution 2D, MaxPool2D, Flatten, Dropout, and Dense, as the foundation for constructing the CNN structure. These classes play a crucial role in defining the architecture of the Convolutional Neural Network (CNN) used in the study. In each convolutional layer, the filter sizes used are 3, 32, 64, 128, and 256, and the Rectified Linear Unit (ReLU) activation function is applied. The ReLU activation function is chosen for its ability to introduce non-linearity to the model and avoid the vanishing gradient problem. As for the final Dense layer, the Softmax activation function is used. Softmax is commonly employed for multiclass classification tasks, where the output layer contains more than one neuron. It allows for the computation of class probabilities, making it suitable for determining the most likely class among multiple classes (Krizhevsky, 2012).

RESULT AND DISCUSSION

Data Augmentation

In the initial stage of the research, data preprocessing was performed, aiming to standardize the format of the input data and expand the data variations. In this study, scaling with a factor of 1/225 and horizontal flipping were utilized for data standardization. An example of the augmented image resulting from this process is shown in Fig. 1.

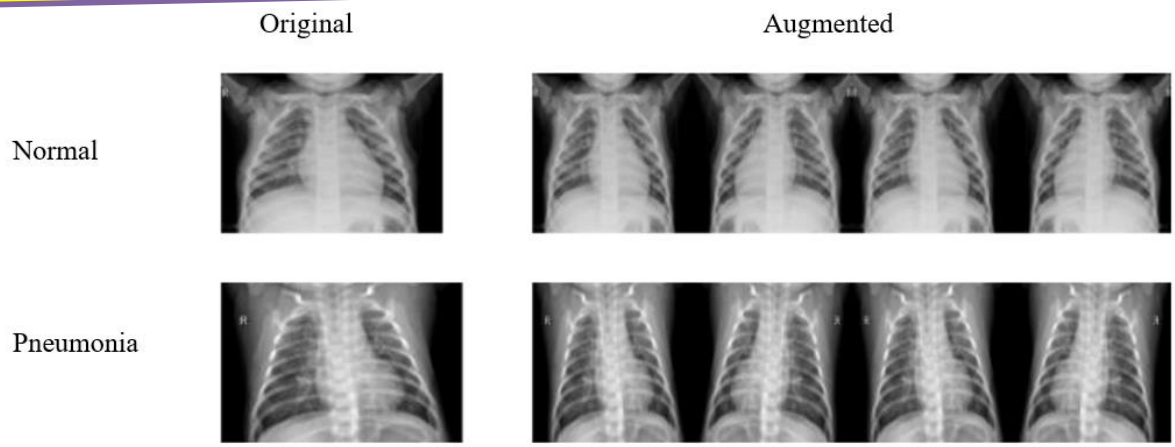

FIGURE 1. Samples of normal and pneumonia chest x-ray images during the data augmentation process are shown in Fig. 4.

The Convolutional Neural Network (CNN) Model Architecture

In this research, a Convolutional Neural Network (CNN) machine learning model was constructed with the following structure: 6 convolutional layers, 5 MaxPool layers, 1 Flatten layer, 1 Dropout layer, and 2 Dense layers, employing filter sizes of 3, 32, 64, 128, and 256. Unlike previous studies that utilized transfer learning approaches with pre-existing models that could be modified as needed, this research manually designed the model. Each layer was meticulously considered for its function and efficiency, utilizing modules from the Keras API to facilitate the process for each layer.

Results of the Model Classification

The research was conducted using 20 epochs for each input variation, namely input sizes of 150x150 pixels, 180x180 pixels, and 200x200 pixels. The accuracy values obtained from the training and testing processes by the CNN model are presented in TABLE 1.

TABLE 1. Comparison of Training and Testing Accuracy Result

Input Size	**Training Accuracy**	**Testing Accuracy**
150x150	72%	80%
180x180	74%	80%
200x200	77%	80%

TABLE 1 illustrates the accuracy performance in both the training and testing processes of the CNN model for each testing scenario with different input image sizes. Each scenario was run for 20 epochs. The values in TABLE 1 were obtained by executing the eval command provided by Keras TensorFlow.

In the first scenario, the image size was set to 150x150 pixels as input to the model. The accuracy achieved was 72% for training and 80% for testing. The model's performance with an input size of 150x150 pixels during the training process can be observed in FIGURE 2.

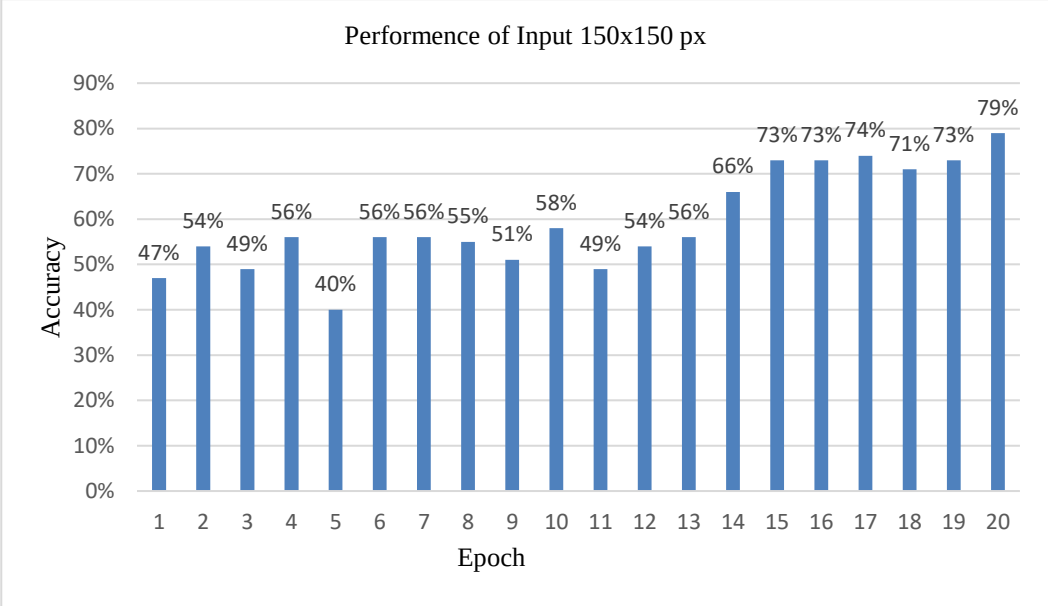

FIGURE 2. Accuracy Graph against Epochs for Input 150x150 Pixels

In the second scenario, the image size was set to 180x180 pixels as input to the model. The accuracy achieved was 74% for training and 80% for testing. The model's performance with an input size of 180x180 during the training process can be observed in FIGURE 3.

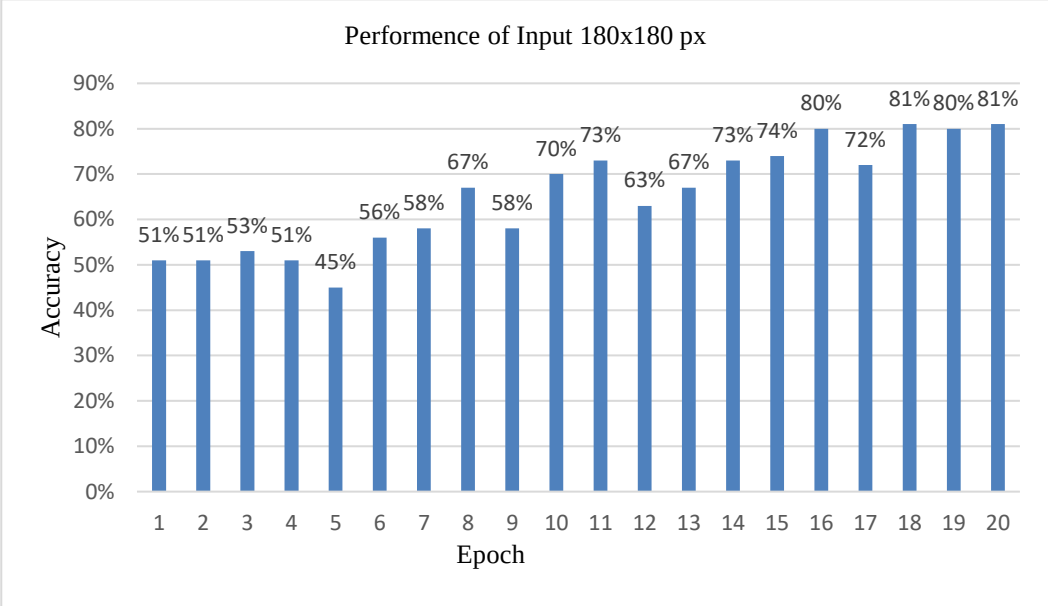

FIGURE 3. Accuracy Graph against Epochs for Input 180x180 Pixels

In the third scenario, the image size was set to 200x200 pixels as input to the model. The accuracy achieved was 77% for training and 80% for testing. The model's performance with an input size of 200x200 pixels during the training process can be observed in FIGURE 4.

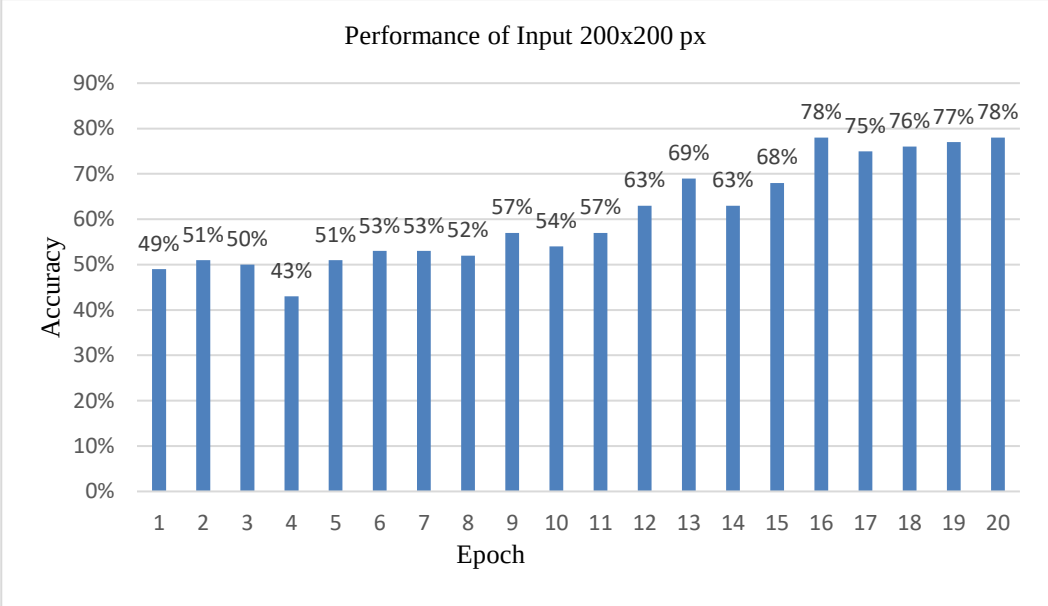

FIGURE 4. Accuracy Graph against Epochs for Input 200x200 Pixels

From the obtained accuracy data, it can be observed that the model produces stable accuracy values with the three different input sizes, yielding 80% accuracy during testing. The efficiency of the model's execution time can be seen in TABLE 2.

TABLE 2. Average Processing Time per 1 Epoch

Input Size (Pixels)	Average Processing Time (ms/epoch)
150x150	11.95
180x180	9.6
200x200	17.2

The fastest average time required for the model to complete one epoch was obtained with an input size of 180x180 pixels, which took 9.6 ms/epoch. This indicates that the model exhibits efficient processing speed. The prediction results for the test data, with a total of 160 samples consisting of 80 Pneumonia and 80 normal images, were compared to the confusion matrix table as show in TABLE 3.

TABLE 3. Confusion Matrix Table for Training - Input 150x150 Pixels

		Doctors Diagnose Result	
		Pneumonia	Normal
Programs Result	Pneumonia	57.6	22.4
	Normal	22.4	57.6

TABLE 4. Confusion Matrix Table for Training - Input 180x180 Pixels

		Doctors Diagnose Result	
		Pneumonia	Normal
Programs Result	Pneumonia	59.2	20.8
	Normal	20.8	59.2

TABLE 5. Confusion Matrix Table for Training - Input 200x200

		Doctors Diagnose Result	
		Pneumonia	Normal
Programs Result	Pneumonia	61,6	18,4
	Normal	18,4	61,6

TABLE 6. The Results of Accuracy, Sensitivity, and Specificity Calculation for Training

Input Size (Pixels)	Accuracy (%)	Sensitivity (%)	Specify (%)
150x150	0,72	0,72	0,72
180x180	0,74	0,74	0,74
200x200	0,77	0,77	0,77

Meanwhile, for the testing calculation, a single Confusion Matrix was utilized because the number of data and the accuracy generated by the model were the same for all three experimental scenarios. The dataset consisted of 20 samples, with an equal distribution of 10 pneumonia and 10 normal images, and input sizes of 150x150 pixels, 180x180 pixels, and 200x200 pixels.

TABLE 7. Confusion Matrix Table – Testing Result

		Doctors Diagnose Result	
		Pneumonia	Normal
Programs Result	Pneumonia	8	2
	Normal	2	8

TABLE 8. Confusion Matrix Table – Testing Result

Input Size	Accuracy (%)	Sensitivity (%)	Specify (%)
150^2, 180^2, and 200^2	0,8	0,8	0,8

From the conducted experiments, it can be observed that the input size with the highest accuracy during the training process is the input size of 200x200 pixels, achieving an accuracy rate of 77%. There is a significant difference of 4% between the input sizes of 150x150 pixels and 200x200 pixels, and 3% between 180x180 pixels and 200x200 pixels. Meanwhile, during the testing process, all three scenarios achieved the same accuracy rate of 80%. Subsequently, an experiment beyond the scope of the research was conducted by running the training command for a second time, i.e., using 40 epochs. The results showed that with an input size of 150x150 pixels, the model achieved an accuracy of 95%, while for 180x180 and 200x200 px, the model experienced overfitting. In the case of overfitting, the model obtained perfect accuracy during training but significantly lower accuracy during testing, indicating the model's inability to recognize features beyond the training data. The prediction results of the model in this study were satisfactory, even though the model was manually constructed by assembling the CNN layers one by one according to their respective functions, rather than using transfer learning approaches. The model provided accurate predictions for data outside the training, testing, and validation datasets, correctly classifying pneumonia as [0,1] and normal as [0,0]. The code and results are available in the appendix. It can be concluded that the model in this study can classify pneumonia and normal chest X-ray images similar to transfer learning methods in previous research. However, further optimization is required to improve the accuracy and enhance stability.

CONCLUSION

The CNN model achieved an accuracy of 80% on the test data for all three input sizes. However, on the training data, it achieved accuracy of 72% for 150x150 pixels, 74% for 180x180 pixels, and 77% for 200x200 pixels. For the 150x150 pixels input, the model reached a maximum accuracy of 95% when trained for 40 epochs, but it experienced overfitting for the 180x180 pixels and 200x200 pixels inputs. Regarding the sensitivity and specificity values, the training results in this study showed sensitivity and specificity of 72% for the 150x150 pixels input, 74% for 180x180 pixels, and 77% for 200x200 pixels. However, during testing, all three input scenarios had the same sensitivity and specificity values, which were both 80%.

ACKNOWLEDGMENTS

I express my gratitude to Lecturers in Physics Department Faculty of Science and Technology Universitas Airlangga for the opportunity to submit our paper.

REFERENCES

1. Allaouzi, I., & Ahmed, M. B. (2019). A novel approach for multi-label chest X-ray classification of common thorax diseases. *IEEE Access, 7*, 64279-64288.
2. Bharati, S., Podder, P., & Hossain, R. (2020). Hybrid deep learning for detecting lung diseases from X-ray images. *Journal of Informatics in Medicine Unlocked, 20*(2020). Publisher: Elsevier.
3. Chollet, F. (2015). Keras. Retrieved December 27, 2022, from https://keras.io.
4. Firmansyah, I., Hayadi, B. H. (2022). Komparasi Fungsi Aktivasi Relu Dan Tanh Pada Multilayer Perceptron. *JIKO: Jurnal Teknik Energi Elektrik, Teknik Telekomunikasi, & Teknik Elektronika, 8*(2), 200-206. September 2022.
5. Franquet, T. (2018). Imaging of community-acquired pneumonia. *Journal of Thoracic Imaging*.
6. Geitgey, A. (n.d.). Machine Learning is Fun Part 3: Deep Learning and Convolutional Neural Networks. Retrieved December 27, 2022, from https://medium.com/@ageitgey/machine-learning-is-fun-part-3-deep-learning-and-convolutional-neural-networks-f40359318721.
7. Hariyani, Y. S., et al. (2020). Deteksi Penyakit Covid-19 Berdasarkan Citra X-Ray Menggunakan Deep Residual Network. *ELKOMIKA: Jurnal Teknik Energi Elektrik, Teknik Telekomunikasi, & Teknik Elektronika, 8*(2), 443-453. May 2020.
8. Heidari, M., Mirniaharikandeheia, S., Khuzanib, A.Z., Danalaa, G., Qiu, Y., & Zheng, B. (2020). Improving the performance of CNN to predict the likelihood of COVID-19 using chest X-ray images with preprocessing algorithms. *International Journal of Medical Informatics, 144*, 104284. December 2020. Publisher: Elsevier.
9. Howard, A., Sandler, M., Chu, G., Chen, L. C., Chen, B., Tan, M., ... & Le, Q. V. (2019). Searching for mobilenetv3. *Proceedings of the IEEE International Conference on Computer Vision* (pp. 1314-1324).
10. Huang, C., Wang, Y., Li, X., Ren, L., Zhao, J., Hu, Y., … Cao, B. (2020). Clinical features of patients infected with 2019 novel coronavirus in Wuhan, China. *The Lancet, 395*(10223), 497–506